MODELING OF FLUID FLOW INSIDE UMP'S FRANCIS TURBINE USING COMPUTATIONAL FLUID DYNAMICS (CFD)

MUHAMMAD NUR IZNEI BIN HASHIM

Thesis submitted in fulfilment of the requirements
for the award of the degree of
Bachelor of Mechanical Engineering

Faculty of Mechanical Engineering
UNIVERSITY MALAYSIA PAHANG

NOVEMBER 2009

SUPERVISOR'S DECLARATION

I hereby declare that I have checked this project and in my opinion, this project is adequate in terms of scope and quality for the award of the degree of Bachelor of Mechanical Engineering.

Signature

Name of Supervisor   : DEVARAJAN A/L RAMASAMY

Position   : LECTURER

Date   : 23 NOVEMBER 2009

STUDENT'S DECLARATION

I hereby declare that the work in this project is my own except for quotations and summaries which have been duly acknowledged. The project has not been accepted for any degree and is not concurrently submitted for award of other degree.

Signature

Name   : MUHAMMAD NUR IZNEI BIN HASHIM

ID Number   : MA06017

Date   : 26 NOVEMBER 2009

ACKNOWLEDGEMENTS

ABSTRACT

This project describes and explains the fluid flow conditions and parameters within a Francis Turbine with regards to each part of the turbine in contact with the working fluid and all working parts of the turbine. The process of obtaining the fluid flow condition and characteristic within the turbine is done by Computational Fluid Dynamics (CFD) simulation. Before CFD simulation is done, a model of the Francis needs to be selected as there are wide ranges of model ranging from conventional usage to demonstration purposes. Considering the availability of the turbine and data, UMP's Gunt Hamburg Demonstration Francis Turbine HM150.20 was selected. The project was then continued by referring to this model. The project was divided into 3 main parts that is experiment on the actual Francis Turbine in order to get real data which will then be used to validate the simulation data by the mean of comparing efficiency curve. The next part is Computer Aided Design (CAD) modeling based on the Gunt Hamburg Demonstration Francis Turbine HM150.20 dimensions and specifications obtained from the manufacturer and measurement on the actual turbine. The CAD modeling was done with consideration to the working parts of the turbine and external parts which are not bounded by the fluid flow region are placed with equivalent readout such as torque which is measured directly at the runner. The third part of the project would be the simulation by using CFD code. During this part, the constructed CAD model is subjected to boundary and flow conditions obtained from experiment and run to obtain the required data. After simulation is done by CFD code, the data obtained is validated by comparing the efficiency curve to verify that the simulation result is correct and fulfill the condition needed for analysis. The significance of the project is that it provides comprehensive and complete flow condition within UMP's Gunt Hamburg Demonstration Francis Turbine HM150.20 which can be used for further studies on the fluid flow inside the turbine and efficiency improvement for the turbine.

ABSTRAK

Projek ini menceritakan dan menerangkan keadaan pergerakan dan parameter bendalir di dalam "Francis Turbine" dengan perihal bahagian-bahagian yang berada dalam lingkungan bendalir dan bahagian operasi "Turbine" tersebut. Proses mendapatkan pergerakan bendalir dan karakteristik dilakukan melalui Pengiraan Bendalir Dinamik (CFD). Sebelum CFD dilakukan, model "Francis Turbine" harus dipilih terlebih dahulu kerana terdapat seleksi "Francis Turbine" yang besar dari jenis conventional ke jenis demonstrasi. Berdasarkan seleksi data dan "Francis Turbine" yang sedia ada, Gunt Hamburg Demonstration Francis Turbine HM150.20 UMP dipilih. Projek ini terbahagi kepada 3 bahagian iaitu experimentasi ke atas "Francis Turbine" bagi mendapatkan data yang akan digunakan bagi mengesahkan data yang bakal diperolehi dari simulasi. Kemudian process memodel "Francis Turbine" melalui Rekaan Bantuan-Komputer (CAD) berdasarkan spesifikasi yang diperoleh dari pengeluar dan ukuran yang diperolehi dari "Turbine" tersebut. Ketiga ialah proses simulasi melalui kod CFD. Ketika bahagian ini, model CAD yang dibina disimulasi dengan keadaan sempadan dan pergerakan bendalir yang diperoleh dari eksperimen untuk mendapatkan data yang deiperlukan. Selepas simulasi dilakukan oleh kod CFD, data melaui proses pengesahan melalui perbandingan bentuk lengkung keberkesanan simulasi dan eksperimen bagi memastikan ianya betul dan memenuhi keadaan diperlukan untuk analysis pergerakan bendalir. Signifikasi projek ini ialah ia membekalkan keadaan pergerakan bendalir yang komprehensif dan lengkap didalam Gunt Hamburg Demonstration Francis Turbine HM150.20 UMP yang boleh digunakan untuk kajian akan datang mengenai pergerakan bendalir di dalam "Turbine" disamping penambahbaikkan keberkesanan "Turbine" tersebut.

TABLE OF CONTENT

CHAPTER 1   INTRODUCTION

CHAPTER 2   LITERATURE REVIEW

LIST OF TABLES

LIST OF FIGURES

LIST OF ABBREVIATIONS

Ŋ	Efficiency
2-D	2-Dimensional
3-D	3-Dimensional
CAD	Computer Aided Design
CFD	Computational Fluid Dynamics
F	Force
H	Head (Pressure)
K-ϵ	K-Epsilon
LBM	Lattice Boltzmann Method
LES	Large Eddy Simulation
M	Torque
n	Speed
P_{ab}	Braking Power
P_{hyd}	Hydraulic Power
RANS	Reynolds-Averaged Navier-Stokes
SPH	Smoothed Particle Hydrodynamics

CHAPTER 1

INTRODUCTION

1.1 INTRODUCTION

Francis turbine is a type of hydropower reaction turbine that contains a runner that has water passages through it formed by curved vanes or blades. The runner blades, typically 6 to 19 in number, cannot be adjusted. As the water passes through the runner and over the curved surfaces, it causes rotation of the runner. The rotational motion is transmitted by a shaft to a generator. It is an inward flow reaction turbine that combines radial and axial flow concepts where both concepts are flow are integrated into the turbine in order to make the water flow within the generator to be able to generate highly efficient rotation and energy transfer to the shaft and runners.

Francis Turbine is a hydropower reaction turbine that was discovered and invented by James Bicheno Francis in the year 1848. James Bicheno Francis was a British-American Engineer; he was born in Southleigh, Oxfordshire in England and immigrated to the United States at age 18. In 1834 he got a job at the Locks and Canal Company of Lowell, Massachusetts and became Chief Engineer in 1837 where he there remained at the company for his entire career.

It was in the years 1848 where he made his greatest achievement and contribution to the scientific society where he designed and created Francis Turbine which was a great improvement of the earlier turbines created by Jean-Victor Poncelet, Benoît Fourneyron, and Uriah Atherton Boyden to create a turbine with 90% efficiency which was far greater than what had been achieved by the earlier generation turbines.

He applied scientific principles and testing methods to produce the most efficient turbine design ever. More importantly, his mathematical and graphical calculation methods improved the state of the art of turbine design and engineering. His analytical methods allowed confident design of high efficiency turbines to exactly match a site's flow conditions. The Francis Turbine was considered to be a more efficient successor to the Boyden turbine. His analysis was proven as he opt to use skewed blade which is able to harvest energy from flowing water both radial and axial flow.

1.2 PROJECT OBJECTIVE

There are several objectives that are needed to be completed by the end of this project which are:

1. To create a complete, accurate and working 3D model of UMP's Francis Turbine in CAD.
2. To subject the constructed 3D model of UMP's Francis Turbine to boundary and initial condition such as the working environment of a Francis Turbine so that the fluid flow can be analyzed by a CFD code.
3. To study the flow characteristic of a Francis Turbine by means of analyzing the simulation result and interpreting them into their respective characteristic.

1.3 PROJECT SCOPE

This project concentrates it study on the flow analysis within the turbines runner under similar operating conditions of the actual turbine. Graphical and numerical simulation is done to determine and display the velocity profile and pressure distribution within the turbine runner and use the information to improve the efficiency of the turbine. The scopes of study are as follows:

1. CAD solid modeling (SOLIDWORK)
2. CFD analysis (COSMOS)
3. Turbine parameter modification.
4. Turbine efficiency improvement.
5. Validation study of efficiency and flow characteristic.

1.4 PROJECT BACKGROUND

The purpose of this project is to identify the pressure and velocity profile distribution within the runner of a Francis Turbine. From this project, we can observe and determine the pattern of velocity profile and pressure distribution by using CFD simulation program after the 3D modeling of the Francis Turbine is made.

Before the simulation is started, we need to determine the values of the Francis Turbine's working condition such as its pressure, mass flow rate etc. It is based on these reference values that we apply the values to the CAD model. Besides, our simulation is based on the design of the Francis Turbine. After finish the simulation, we need to devise a method to increase the performance and efficiency of the turbine.

Basically, the project revolves around the idea of investigating the effect and distribution of velocity profile and pressure within a turbine and based on the result obtained from the simulation to improve the turbine's efficiency.

1.5 PROBLEM STATEMENT

In turbines, one of the most important characteristic or properties of hydro powered turbines is the overall efficiency of the turbine which can be translated as how much of the original power of the flowing water is successfully converted or translated into electrical energy in case of damps. Turbines development have been mainly been focused on a creating a well rounded turbine with high efficiency value. However the actual efficiency and performance of this turbine may vary according to ambient conditions and working environment. It's based on this assumption that we are to analyze UMP's Francis Turbine to determine its rated efficiency.

The variation in the calculated efficiency compared to the theoretical efficiency of Francis Turbine occur caused by several factors which is different from the ideal condition of the turbine. Since turbines constructed by the supplier are practically identical, the factors that affect this efficiency difference surely must lay within the turbine's configuration e.g. the guiding vanes angle etc. Next is the existence of

cavitations which reduces the turbine's overall efficiency and at the same time breaks or creates and propagates cracks at the runner's blade thus rendering the turbine defective.

When cavitations occur, the blades on the runner gather bubbles and pop. The pop of the bubbles break and indent the runner and guiding vanes that help the water or fluid move from the middle of the runner to the leading edge of the runner. The sound of cavitations is like pumping gravel through the volute or case. If the pump is experiencing cavitations, the ball valve is slowly turned clockwise to reduce input flow rate on the discharge side of the pump on a centrifugal pump and the gravel noise will reduce as a sign that the cavitations has been reduced. Cavitations will destroy the runner very fast by imploding bubbles on the runner and guiding vanes until the pump will not run anymore.

1.6 PROBLEM SOLVING

To study the flow characteristic of a Francis Turbine, several methods could be used. The easiest would be the path chosen in the project that is to attempt to model the fluid flow inside the turbine itself by mean of CAD modeling and CFD simulation. The method is the easiest and most effective since the variables and condition can be change at ease and the result from the modeling will be presented in both numerical and graphical method.

Several ways can be done to improve of optimize the efficiency of UMP's Francis Turbine; the simple method is to adjust the guiding vanes, so that the angle of entrance is changed and the cavitations is reduced or eliminated from the flow. The more complex method is modifying the turbines geometry and physical properties such as surface roughness, internal diameter, runner diameter etc. However trial and error method for each solution can be wasteful especially if done manually that is through fabrication process. So the best option for analysis is via simulation process which is more effective at testing and less costly. Simulation process which is proposed consist of the first part is the actual model simulation and based on the obtained results, certain parameters will be adjusted for optimum and maximum efficiency of the turbine.

CHAPTER 2

LITERATURE REVIEW

2.1 INTRODUCTION

The purpose of this chapter is to provide a review of the past research related to the current research done which is turbine, Francis Turbine, reaction turbine, cavitations, efficiency, hydro powered turbine, runner, guiding vanes, CAD, CFD, and velocity profile.

2.2 TURBINE

A turbine is a rotary engine that extracts energy from a fluid flow. Claude Burdin coined the term from the Latin *turbo*, or vortex, during an 1828 engineering competition. Benoit Fourneyron, a student of Claude Burdin, built the first practical water turbine.
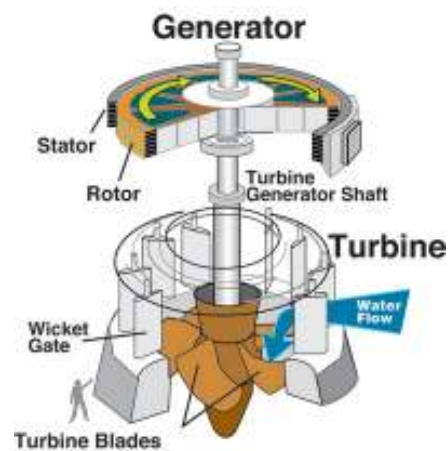
Figure 2.1: A basic electric generating turbine

The simplest turbines have one moving part, a rotor assembly, which is a shaft with blades attached. Moving fluid acts on the blades, or the blades react to the flow, so that they rotate and impart energy to the rotor. Early turbine examples are windmills and water wheels. Gas, steam, and water turbines usually have a casing around the blades that contains and controls the working fluid

2.3 FRANCIS TURBINE

Francis turbine is a type of water turbine that was developed by James B. Francis. It is an inward flow reaction turbine that combines radial and axial flow concepts. Francis turbines are the most common water turbine in use today. They operate in a head range of ten meters to several hundred meters and are primarily used for electrical power production.

Francis turbine was discovered by James Bicheno Francis in 848 by improving the earlier design of Benoit Fourneyron and Jean-Victor Poncelet to yield the most efficient turbine design ever with 90% efficiency.
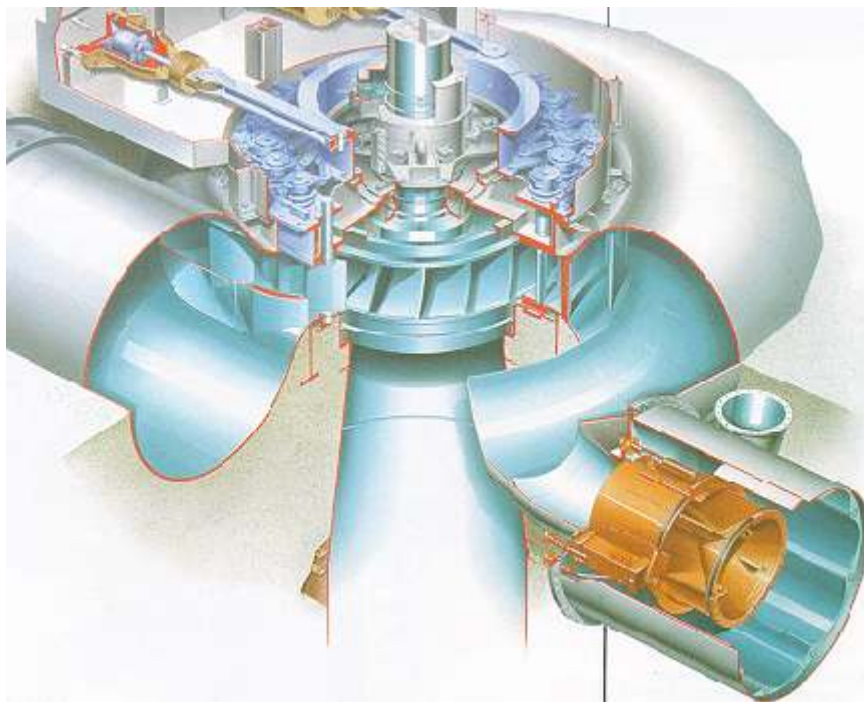
Figure 2.2: A large scale conventional Francis Turbine found in dams

2.4 REACTION TURBINE

These turbines develop torque by reacting to the fluid's pressure or weight. The pressure of the fluid changes as it passes through the turbine rotor blades. A pressure casement is needed to contain the working fluid as it acts on the turbine stage or the turbine must be fully immersed in the fluid. The body of the turbine contains and directs the working fluid and, for water turbines, maintains the suction imparted by the draft tube. Francis turbines and most steam turbines use this concept.

For compressible working fluids, multiple turbine stages may be used to harness the expanding fluid usually gas efficiently. Newton's third law describes the transfer of energy for reaction turbines. "Whenever a particle A exerts a force on another particle B, B simultaneously exerts a force on A with the same magnitude in the opposite direction. The strong form of the law further postulates that these two forces act along the same line. This law is often simplified into the sentence, "To every action there is an equal and opposite reaction."

2.5 CAVITATIONS

Cavitations are the formation of vapor- or gas-filled cavities in liquids. If understood in this broad sense, cavitations includes the familiar phenomenon of bubble formation when water is brought to a boil under constant pressure and the effervescence of champagne wines and carbonated soft drinks due to the diffusion of dissolved gases.

In engineering terminology, the term cavitations is used in a narrower sense, namely, to describe the formation of vapor-filled cavities in the interior or on the solid boundaries created by a localized pressure reduction produced by the dynamic action of a liquid system without change in ambient temperature. Cavitations in the engineering sense is characterized by an explosive growth and occurs at suitable combinations of low pressure and high speed in pipelines; in hydraulic machines such as turbines, pumps, and propellers; on submerged hydrofoils; behind blunt submerged bodies; and in the cores of vertical structures.

This type of cavitations has great practical significance because it restricts the speed at which hydraulic machines may be operated and, when severe, lowers efficiency, produces noise and vibrations, and causes rapid erosion of the boundary surfaces, even though these surfaces consist of concrete, cast iron, bronze, or other hard and normally durable material.

Both experiments and calculations show that with ordinary flowing water cavitations commences as the pressure approaches or reaches the vapor pressure, because of impurities in the water. These impurities, called cavitations nuclei, cause weak spots in the liquid and thus prevent it from supporting higher tensions. The exact mechanism of bubble growth is generally described by mathematical relationships which depend upon the cavitations nuclei.

Cavitations commences when these nuclei enter a low-pressure region where the equilibrium between the various forces acting on the nuclei surface cannot be established. As a result, bubbles appear at discrete spots in low-pressure regions, grow quickly to relatively large size, and suddenly collapse as they are swept into regions of higher pressure.

Figure 2.3: Example of cavitations in Francis Turbine

2.6 EFFICIENCY

The efficiency rated on a Francis Turbine is considered to be mechanical since the operating principle of a Francis Turbine includes the concept of simple mechanical structures such as the water hitting the runner will cause the runner to spin and at the same time rotating the shaft connecting the dynamo (in the case of a damp) to the turbine. This principle of energy transfer through the rotating of shaft is identified as mechanical hence evaluating the efficiency as mechanical.

In physics, mechanical efficiency is the effectiveness of a machine and is defined as:

$$Mechanical\ Efficiency = \frac{Work\ Output}{Work\ Input}$$

(2.1)

Mechanical Efficiency is the ratio of work input to work output. It is often expressed as a percentage. The efficiency of an ideal machine is 100 percent but an actual machine's efficiency will always be less than 100% because of the Second law of thermodynamics which states that the quality of energy will decay, eventually becoming heat. This means that some of the work put into the system is transformed (lost) into thermal energy (heat). In a mechanical system, friction is the most common cause of the work lost to heat.

The actual mechanical advantage of a system is always less than the ideal mechanical advantage due to these losses. Another way to express mechanical efficiency is it is the ratio of actual mechanical advantage to ideal mechanical advantage. In Francis Turbine case, the efficiency is the ratio of the power output or the braking force, to the water power entering the turbine.

2.7 RUNNER

In a Francis Turbine, the runner is the part of the turbine which is connected directly to the shaft of the turbine which is then normally connected to the dynamo. The runner consists of several small blades or fins which accepts and enhances the energy transfer from moving water to the shaft. The runner then, with the help of this blades spins based on the water flows energy which is successfully transferred to runner.
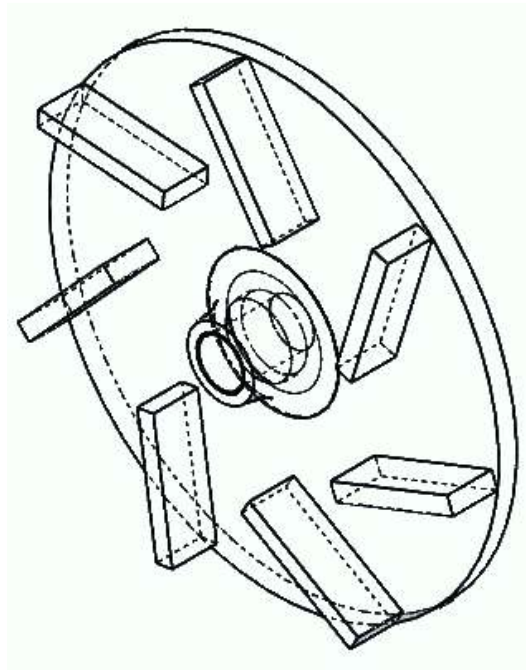
Figure 2.4: CAD model of the Gunt Hamburg Francis turbine runner

Since a Francis Turbine is inward flow reaction turbine, the runner is located at the centre at the turbine with a small cylindrical rod with curved sides at the very centre of the turbine which helps the water flow out of the turbine after their energy is transferred via the runner to the shaft. The water usually enters the runner at an angle somewhat tangential to the blades on the runner to gather the most energy from the flowing water. The runner of a Francis Turbine is said to be the most efficient turbine design up to date.

2.8 GUIDING VANES

The guiding vanes of a Francis Turbine are curved aerofoil-like parts of the Francis Turbine which normally placed at a certain distance away from the runner and consist of several parts which surrounds the runner. These vanes are used mainly for two reasons. The first is to guide the flowing working fluid to the runner and to control the angle of entrance so that cavitations will be reduced or eliminated.
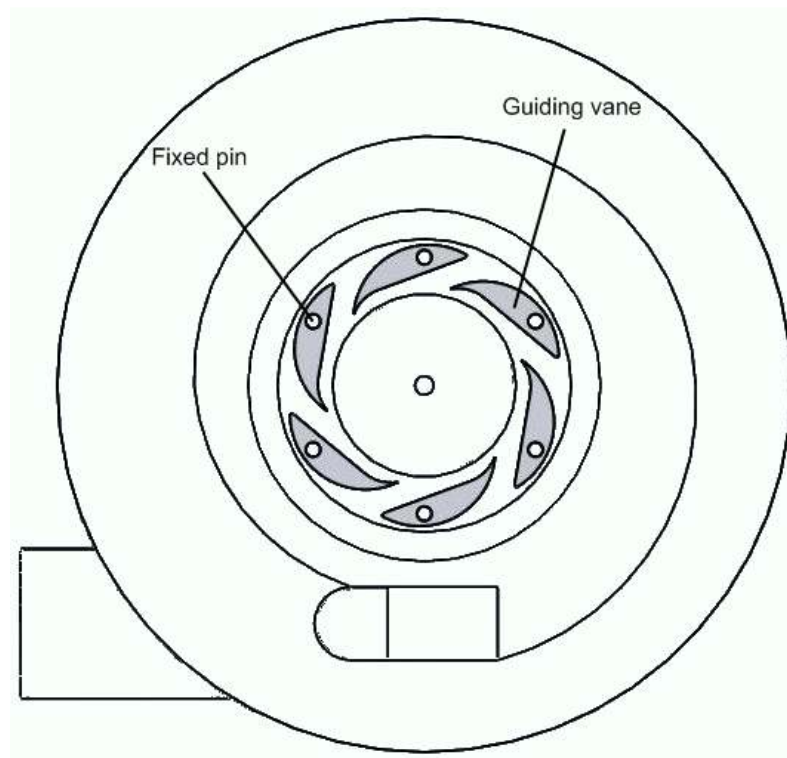
Figure 2.5: CAD model of the Gunt Hamburg Francis turbine guiding vanes and its position on the Francis Turbine

The vanes are placed so that the flowing water which enters the turbine is redirected into the passage created by the vanes. Water that flows within the Francis Turbine are classified as turbulent which mean their flows are highly unsteady and violent. It is the characteristic of this flow that cause the water inside the turbine to

bounce on the turbine wall which then flows in all direction and then is guided by the guiding vanes straight into the runner.

For the second function, the guiding vanes are built with a pin near the end of the vanes so that the vanes will be adjustable in order to reduce the formation of cavitations. Usually the optimum angle in which the flow of the working fluid will not produce any cavitations is around 20°-30°. However, this angle varies upon the working fluids flow.

2.9 COM PUTER-AIDED DESIGN (CAD)

Computer-Aided Design (CAD) is the use of computer technology to aid in the design and particularly the drafting (technical drawing and engineering drawing) of a part or product, including entire buildings. It is both a visual (or drawing) and symbol-based method of communication whose conventions are particular to a specific technical field. Drafting can be done in two dimensions (2D) and three dimensions (3D).

Drafting is the communication of technical or engineering drawings and is the industrial arts sub-discipline that underlies all involved technical endeavors. In representing complex, three-dimensional objects in two-dimensional drawings, these objects have traditionally been represented by three projected views at right angles. CAD is used in the design of tools and machinery and in the drafting and design of all types of buildings, from small residential types (houses) to the largest commercial and industrial structures (hospitals and factories).

CAD is mainly used for detailed engineering of 3D models and/or 2D drawings of physical components, but it is also used throughout the engineering process from conceptual design and layout of products, through strength and dynamic analysis of assemblies to definition of manufacturing methods of components. CAD has become an especially important technology within the scope of computer-aided technologies, with benefits such as lower product development costs and a greatly shortened design cycle.

CAD enables designers to dish out and develop work on screen, print it out and save it for future editing, saving time on their drawings.

CAD is used in a variety of ways within engineering companies. At its simplest level it is a 2D Wireframe package that is used to create engineering drawings. This has however over the last 20 years been overtaken by 3D parametric feature based modeling. Component forms are created either using freeform surface modeling or solid modeling or a hybrid of the two. These individual components are then assembled into a 3D representation of the final product; this is called bottom-up design. These assembly models can be used to perform analysis to assess if the components can be assembled and fit together as well as for simulating the dynamics of the product.

2.10 COMPUTATIONAL FLUID DYNAMICS (CFD)

Computational fluid dynamics (CFD) is one of the branches of fluid mechanics that uses numerical methods and algorithms to solve and analyze problems that involve fluid flows. Computers are used to perform the millions of calculations required to simulate the interaction of fluids and gases with the complex surfaces used in engineering. Even with high-speed supercomputers only approximate solutions can be achieved in many cases.

Ongoing research, however, may yield software that improves the accuracy and speed of complex simulation scenarios such as transonic or turbulent flows. Initial validation of such software is often performed using a wind tunnel with the final validation coming in flight test.

The most fundamental consideration in CFD is how one treats a continuous fluid in a discretized fashion on a computer. One method is to discretize the spatial domain into small cells to form a volume mesh or grid, and then apply a suitable algorithm to solve the equations of motion (Euler equations for inviscid and Navier-Stokes equations for viscous flow). In addition, such a mesh can be either irregular (for instance consisting of triangles in 2D, or pyramidal solids in 3D) or regular; the distinguishing characteristic of the former is that each cell must be stored separately in memory.

If one chooses not to proceed with a mesh-based method, a number of alternatives exist, notably the smoothed particle hydrodynamics (SPH), a Lagrangian method of solving fluid problems, spectral methods, a technique where the equations are projected onto basis functions like the spherical harmonics and Chebyshev polynomials, lattice Boltzmann methods (LBM), which simulate an equivalent macroscopic system on a Cartesian grid, instead of solving the macroscopic system (or the real microscopic physics).

In SPH the equation for any quantity A at any point r is given by the equation

$$A(r) = \sum_j m_j \frac{A_j}{\rho_j} W(|r - r_j|, h),$$ 2.2

Where

m_j is the mass of particle j,

A_j is the value of the quantity A for particle j,

ρ_j is the density associated with particle j,

r denotes position and

W is the kernel function mentioned above.

Calculation in Lagrangian refers to the introduction of a new variable (λ) called a Lagrange multiplier, and study the Lagrange function defined by

$$\Lambda(x, y, \lambda) = f(x, y) + \lambda \cdot (g(x, y) - c)$$ 2.3

Where λ may be either added or subtracted. If (x,y) is a maximum for the original constrained problem, then there exists a λ such that (x,y,λ) is a stationary point for the Lagrange function (stationary points are those points where the partial derivatives of Λ are zero). However, not all stationary points yield a solution of the original problem. Thus, the method of Lagrange multipliers yields a necessary condition for optimality in constrained problems.

Where as in the study of differential equations they arise as the solution to the Chebyshev differential equations:

$$(1 - x^2)y'' - xy' + n^2y = 0 \qquad (2.4)$$

And

$$(1 - x^2)y'' - 3xy' + n(n + 2)y = 0 \qquad (2.5)$$

for the polynomials of the first and second kind,

Where as in the Boltzmann equation it is an evolution of equation for a single particle probability distribution function $f(x,v,t)$:

$$\partial_t f + v\partial_x f + F\partial_v f = \Omega \qquad (2.6)$$

where F is an external force and Ω is a collision integral.

The lattice Boltzmann method discretizes this equation by limiting space to a lattice and the velocity space to a discrete set of velocities v_i. The discretized Boltzmann equation, which is the Lattice Boltzmann equation, then reads:

$$f_i(x + v_i + 1) - f(x, t) + F_i = \Omega \qquad (2.7)$$

The collision operator is often approximated by a BGK collision operator:

$$\Omega = \frac{1}{\tau}(f_i^0 - f_i) \qquad (2.8)$$

Where f_i^0 is the local equilibrium distribution.

It is possible to directly solve the Navier-Stokes equations for laminar flows and for turbulent flows when all of the relevant length scales can be resolved by the grid (a Direct numerical simulation). In general however, the range of length scales appropriate

to the problem is larger than even today's massively parallel computers can model. In these cases, turbulent flow simulations require the introduction of a turbulence model. Large eddy simulations (LES) and the Reynolds-averaged Navier-Stokes equations (RANS) formulation, with the k-ε model or the Reynolds stress model, are two techniques for dealing with these scales.

In many instances, other equations are solved simultaneously with the Navier-Stokes equations. These other equations can include those describing species concentration (mass transfer), chemical reactions, heat transfer, etc. More advanced codes allow the simulation of more complex cases involving multi-phase flows, non-Newtonian fluids, or chemically reacting flows.

2.11 VELOCITY PROFILE

Not all fluid particles travel at the same velocity within a pipe. The shape of the velocity curve (the velocity profile across any given section of the pipe) depends upon whether the flow is laminar or turbulent. If the flow in a pipe is laminar, the velocity distribution at a cross section will be parabolic in shape with the maximum velocity at the center being about twice the average velocity in the pipe.

In turbulent flow, a fairly flat velocity distribution exists across the section of pipe, with the result that the entire fluid flows at a given single value. The Figure 2.6 helps illustrate the above ideas. The velocity of the fluid in contact with the pipe wall is essentially zero and increases the further away from the wall.
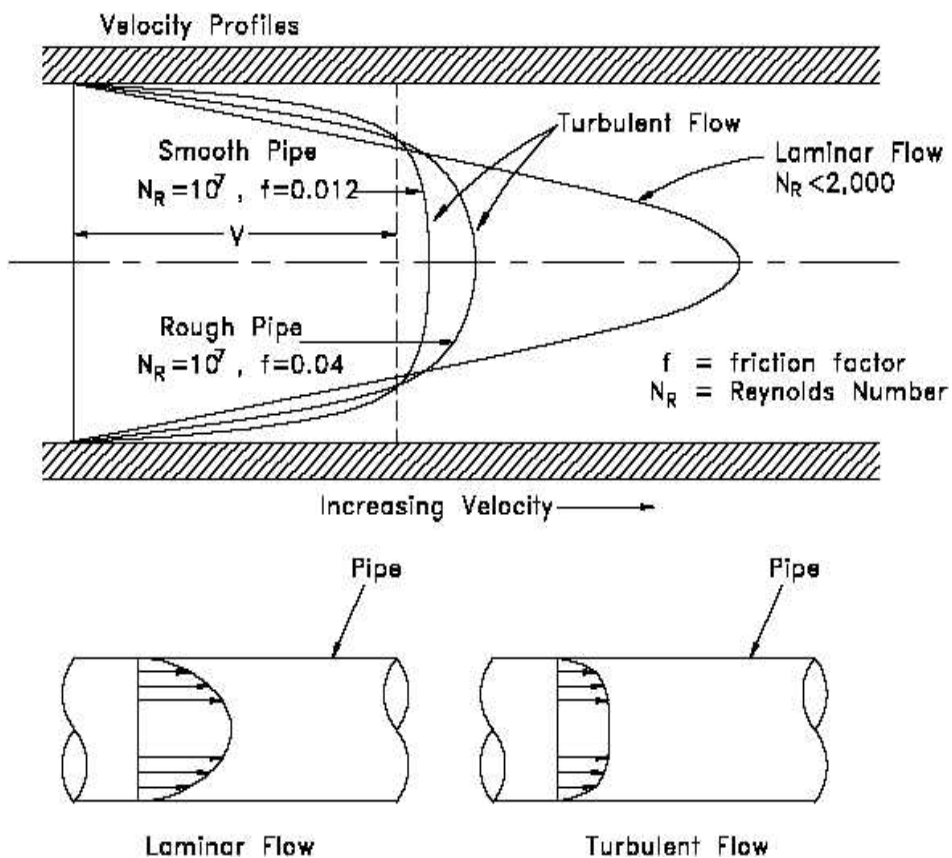
Figure 2.6: Velocity profile diagram for internal flow for laminar and Turbulent Flow Velocity Profiles

Note that from the Figure 2.6 that the velocity profile depends upon the surface condition of the pipe wall. A smoother wall results in a more uniform velocity profile than a rough pipe wall.

CHAPTER 3

METHODOLOGY

3.1 INTRODUCTION

In this chapter, we will be discussing on the methods involved during the course of this project and the processes in which the results and data is obtained. This chapter will give explanation on the methods as well as flow chart diagram, conceptual study, design method, experimental and simulation setup. For the experimental technique are discussed in this chapter.

3.2 FLOW CHART

3.2.1 Flow chart of the study for PSM 1
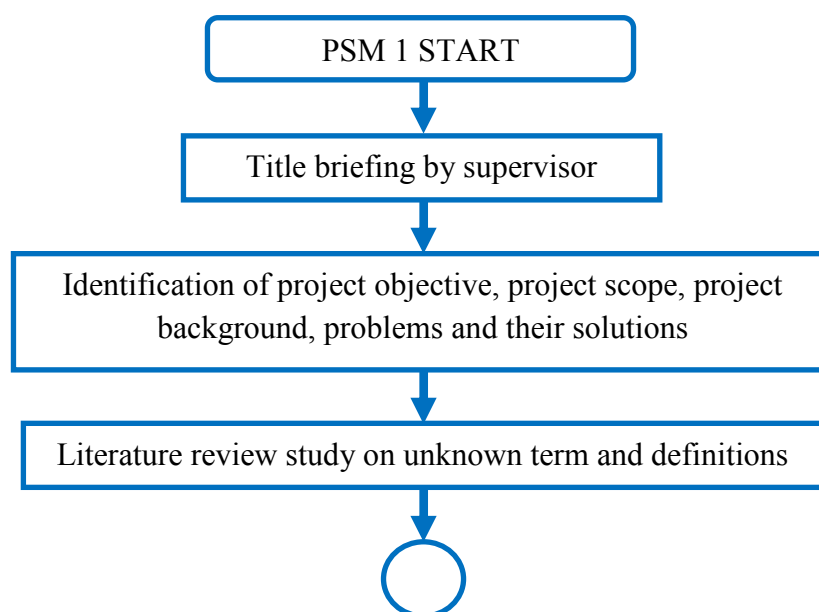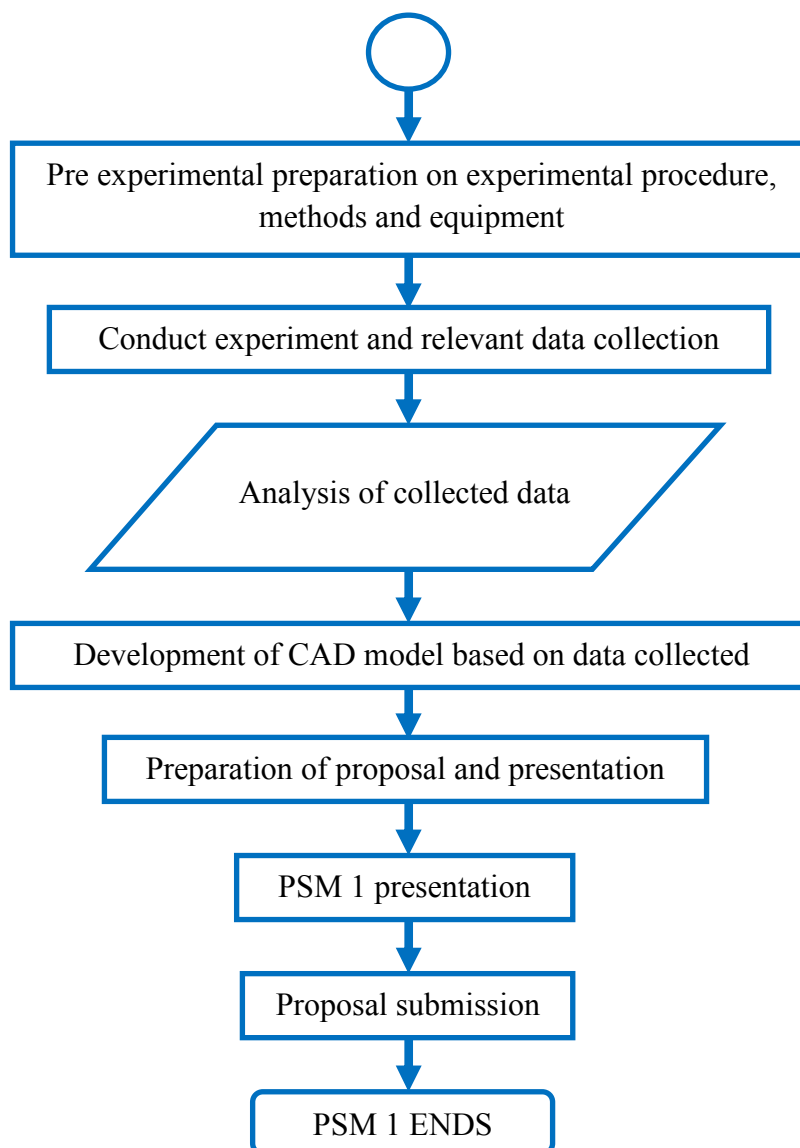
Figure 3.1: Flow chart of the study for PSM 1

3.2.2 Flow chart of the study for PSM 2
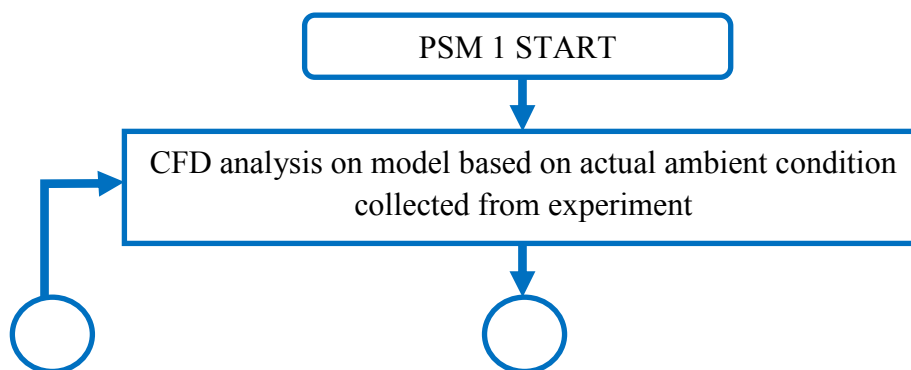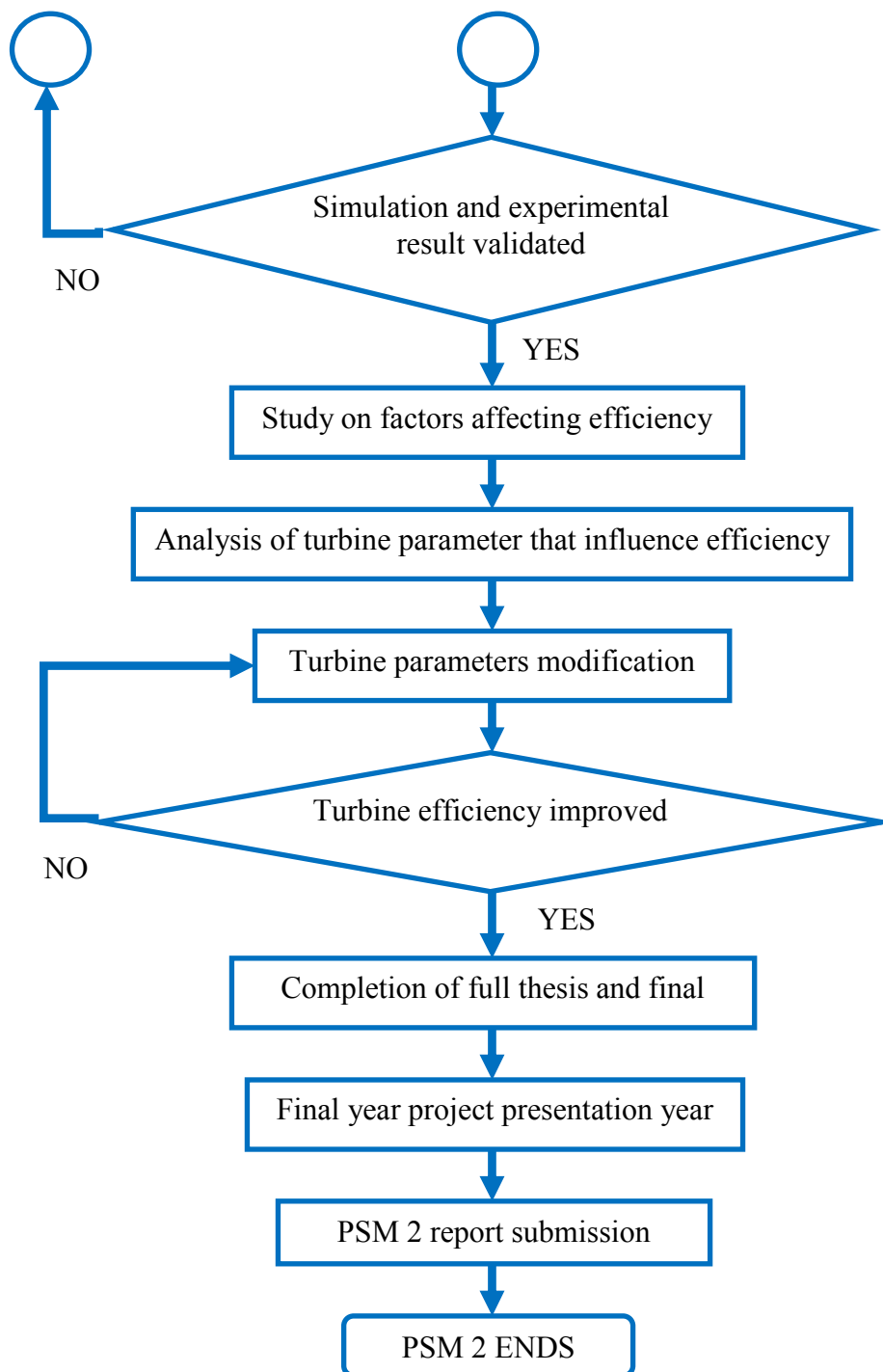
Figure 3.2: Flow chart of the study for PSM 2

3.3 MODEL SELECTION

For modeling and experimental purposes, the GUNT HAMBURG HM 150.20 demonstration Francis Turbine was chosen as the test model since the brand is well known for accuracy and reliability. The turbine was selected over the LOTUS Francis Turbine even though the lotus was newer due to several reasons which are the configuration of the LOTUS turbine in term of the placement of its guiding vanes and the adjustability of the working angle of the guiding vanes which is different than normal guiding vanes configuration.
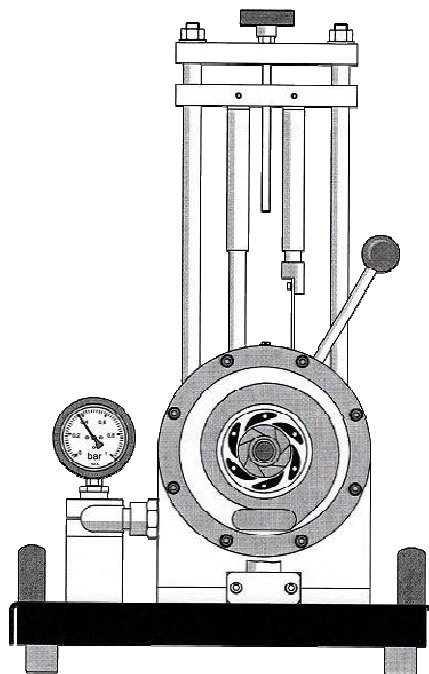
(a)   (b)

Figure 3.3(a) and 3.3(b): Gunt Hamburg HM 150.20 drawing and actual image

3.4 EXPERIMENTAL SETUP

The focus of the experiment in the initial part of the project is mainly on the real turbine itself where we are to measure and study each part of the Francis Turbine and then proceed with manual experimentation to obtain values such as volume flow rate, inlet pressure, rpm and etc. The values will help us in modeling the turbine is CAD and

will be used to analyze the turbines characteristic. This values which is obtained will be calculated where the values will be translated into efficiency characteristic curve, boundary condition for the CFD analysis and several other parameters that will be determined in the next semester if deemed necessary. However, in the advanced stage of the project, he main highlight of the project will be on CFD simulation on the CAD model of the turbine, efficiency curve validation of the results obtained from simulation, and modifications of turbine parameter to improve the turbines efficiency.

3.4.1 Experimentation

3.4.1.1 Pre-experimental Procedure

1. The turbine was cleaned of dirt, and foreign contaminants. The cleaning was made thoroughly including cleaning the internal surface of the turbine which will accommodate flowing water. Plaque build-up which is caused by water composition which includes foreign bodies was cleaned and removed. Grease and lubricant was added to the moving parts of the turbine such as the runner to avoid energy loss due to friction.
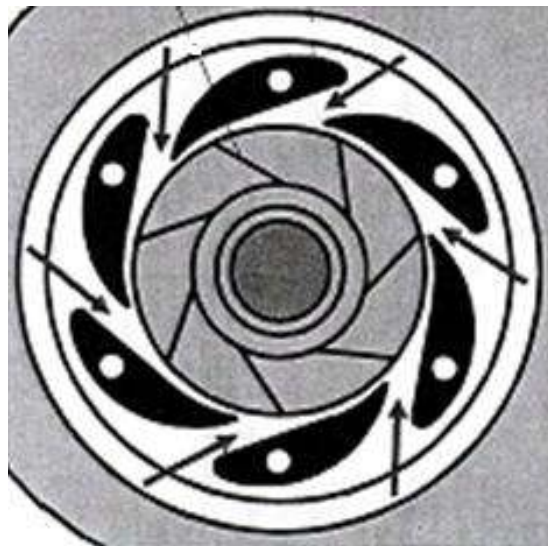
Figure 3.4: Runner and guiding vanes position with arrow representing flow direction

2. The water reservoir was drained and the reservoir tank was cleaned of unwanted dirt and foreign substance. This is to avoid the water flow from being affected by

the substances. Presence of foreign substance can also damage the turbine when water enters the runner and the foreign substance hits the blade of the runner.
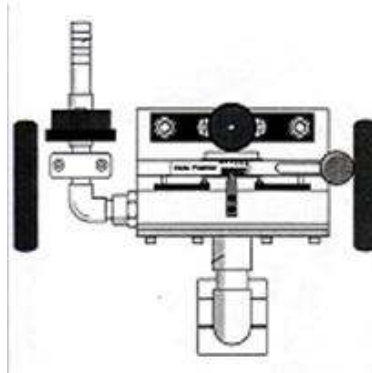
Figure 3.5: Drawing of the pressure gauge and pipe joint which joint the pump work bench to the Francis Turbine

3. The piping and its connection was checked for any leakages and the connection was inspected to make sure that the connection is secured before starting.
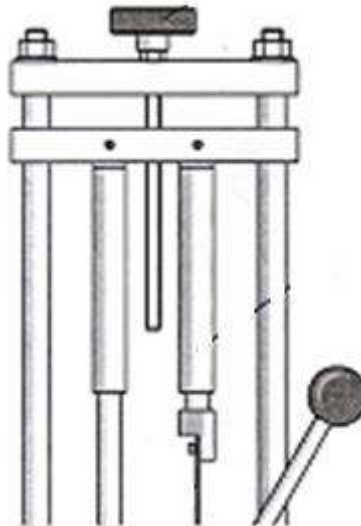
Figure 3.6: Drawing of the braking belts that are attached to the force

4. The apparatus such as the braking belt which supplies the braking force to the turbine was checked for reading consistency and to ensure it is working. The

hand wheel that controls the braking force is also adjusted so that the brake is fully released. The tachometer reading was checked to ensure it able to give legitimate reading and to ensure that it will be able to give stable reading throughout the experimental process.

3.4.1.1 Experiment Procedure

1. Turbine characteristic curve
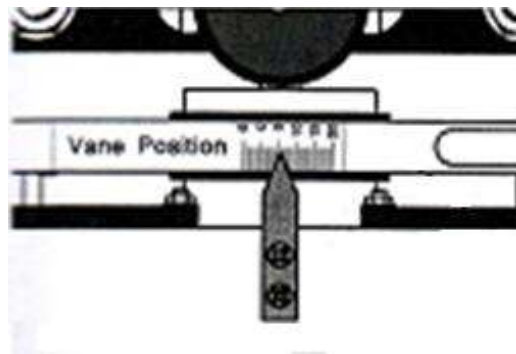
Figure 3.7: Drawing of the vane angle indicator on the Francis Turbine

i.   The guiding vanes were set up to maximum speed position to record turbine characteristic graph. The nominal angle of entrance was set to the usual 10-30°. However, the angle depends on the condition of the outlet flow, if cavities occur the angle needs to be adjusted so that the cavity will be eliminated.
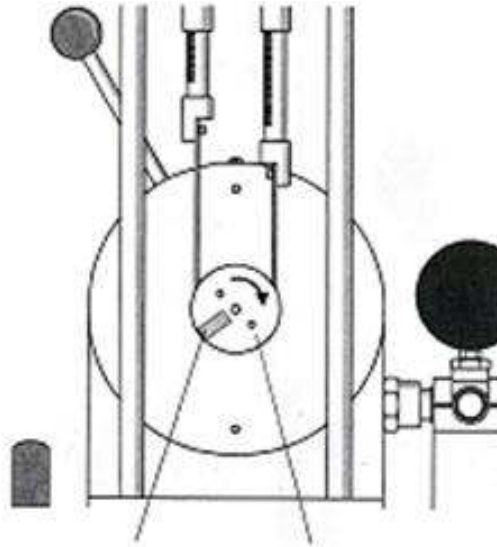
Figure 3.8: Drawing of the pulley with tachometer readout point

ii.   The speed was measured with mounted tachometer which is mounted at the face of the pulley and reads the speed based on the metal object placed on the pulley and the lever was tightened to set the adjustment. The lever was tightened so that the guiding vanes will not move or sway at the power of the flowing water running through the vanes.

iii.   Volumetric flow was set up to ~35 liter/min as described in the HM150 manual. The volume flow rate is measured to be ~35 liter/min, any adjustment need to be done before the experiment is done on the Francis Turbine. The entire series of measurements can be assumed volumetric flow rate as constant. Even though the value in actual does not flow at a constant rate due to the fluctuating pump, the value of the fluctuation is small and can be considered negligible since its effect on the reading is not significant and only occur a small time intervals.
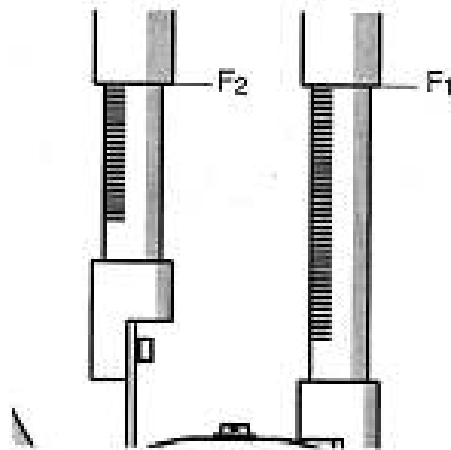
Figure 3.9: Drawing of force readout on the force gauge

iv.   The load at brake or the braking force is increased gradually to reduce the rpm to ~100rpm until the turbines speed declines and the runner finally stops. The braking force is adjusted by rotating the hand wheel on top of the braking unit. The braking force is then measured by calculating the difference between the reading of the right and left hand side force indicated.
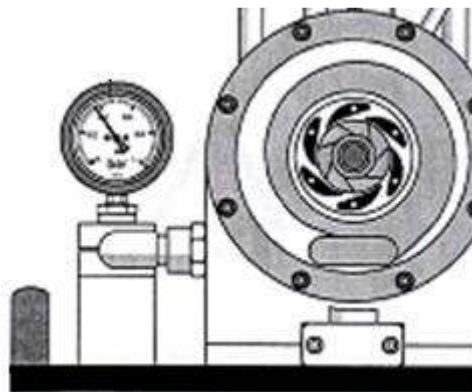
Figure 3.10: Drawing of the pressure gauge with relative to Francis Turbine position

v.   The reading of inlet pressure at each braking force increment is tabulated into a graph. After the braking force is applied and the pressure is stable, the reading of the pressure is taken. The reading was taken after the pressure is

stable because the reading will be biased if taken immediately and to allow the system to properly adjust to the speed change.

2. Determination of flow rate,

i. The pump was turned on and the entire cycle of flowing water was left to flow for several moments. This is to allow the pump to build up its pressure and allow the water cycle to achieve stability before the reading can be taken.

ii. Stop watch was set to zero. This is a pre-caution step to avoid error in reading due to human factors that is unable to response to the nature correctly.

iii. The valve at bottom of volumetric tank is closed using a stopper. This is to measure the volume flow rate of water running from the outlet of the Francis Turbine. This volume flow rate is to be considering constant the entire experiment process and constant in the inlet and outlet of the Francis Turbine.

iv. Wait until the reading on the stop watch has reached 60 second or the water level at the volume indicator reaches 10L then start the stop watch reading. This is to allow the measure to be taken at a stable data and avoid zero error from the water scale.

v. The time readings were taken after the water level has reached 20L and stop the stopwatch afterwards.

vi. 5 readings were taken and an average volume flow rate was calculated.

3.5 COMPUTER-AIDED DESIGN (CAD) MODELLING
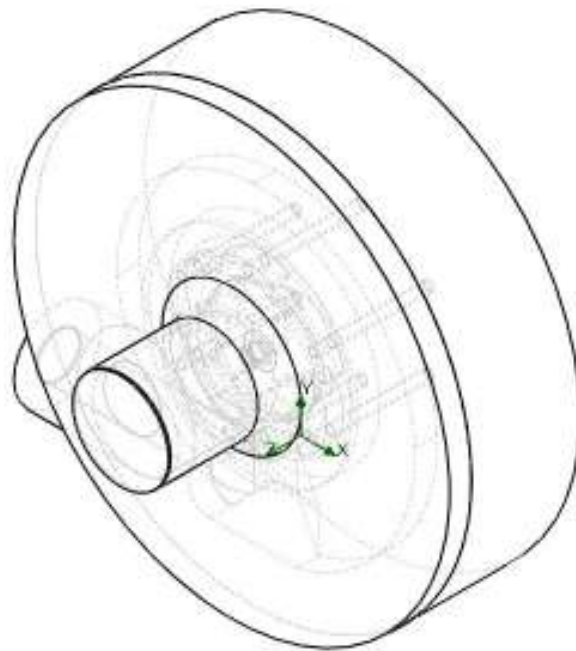
Figure 3.11: Assembled view of the CAD model
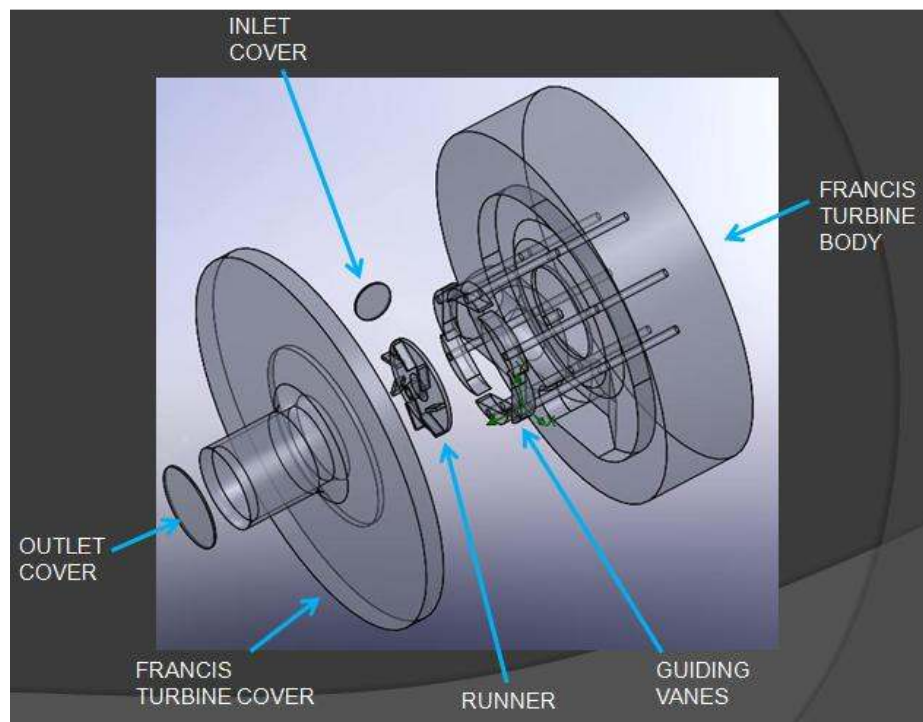
Figure 3.12: Exploded view of the Francis Turbine

3.5.1 Pre-modeling process

1. All relevant dimensions from the working part of the Francis Turbine was analyzed, identified, noted and marked for measurement. This was to avoid excessive measurement of the turbines part and to avoid inadequate dimensions from being recorded. This had also ensured that only the working part of the turbine had been considered into modeling.

2. All tools and equipment needed for the measurement had been identified and noted and borrowed from the laboratory's store. This was done to smoothen the process of measurement and to obtain data with high accuracy and relevant to the CAD model.

3.5.2 Modeling Process

1. Rough sketches were made using the dimensions taken to ensure that the model to be constructed in CAD is well visualize.

2. The Francis Turbine was constructed by parts according to their difficulty and the function of the parts and in the order of modeling is the turbine body, runner and the cover of the turbine.

3. The construction is done by with the dimension provided by the turbine manufacturer and cross-referencing it with the additional dimension obtained by mean of manual measurement on the turbine before experiment process.

4. After each part was constructed, the model is assembled into a complete Francis Turbine and the connection joint condition is checked to assure that it follows the actual working condition of a Francis Turbine.

3.6 COMPUTATIONAL FLUID DYNAMICS (CFD) SIMULATION

1. The assembled Francis Turbine model will be opened in CFD and the simulation project for the simulation will be specified based on criteria identified important in the simulation such as surface roughness, units, fluid, physical feature etc.

2. The connection of the assembly was checked for interference and error to avoid the simulation result from being biased.

3. In order to start the simulation, a new project is specified where the parameters are set.

Table 3.1 Project definition for the simulation

Project name	NEW: Francis Turbine
Unit system	SI
Analysis type	Internal; Exclude cavities without flow conditions
Physical features	Rotation: Type - Global rotating, Rotation axis - Z axis of Global Coordinate system, Angular velocity=0 RPM
Default fluid	Water
Wall Conditions	Adiabatic wall, default smooth walls
Initial Conditions	Default conditions
Result and Geometry Resolution	Set the Result resolution level to 4; Minimum gap size = 0.01 m, minimum wall thickness = 0.01, other options are default

Source: COSMOS Flow simulation

4. Then the boundary condition at the inlet and outlet will be subjected to the model in term of volume or mass flow rate and pressure. These values are obtained from the experimentation. The average value of the volume flow rate was measured during to be 35.0530 l/min and the flow is assumed to have uniform velocity profile with absolute value. The outlet is set to environmental pressure since in actual turbine water from the outlet will flow into open tank. Then is to set the rotating speed of the runner starting from 0 rpm to 1000 rpm with 100 rpm increment as obtained from experiment. The surfaces are selected and the boundary option is selected in order to specify each condition inside the turbine's fluid flow region.

5. Next is the identification of the turbine's body where a part of the turbine remains stationary such as the guiding vanes and internal wall is identified. The

entire fluid contact surface of the turbine is set as stationary except for the runner. To specify the part as fixed, the surfaces are identified as real wall and stator.

6. After that is to specify the project goals and parameter at surfaces and parameters relevant to the study plus the equations for the goals specified. The goals set are at the inlet where the average pressure is measured, at the runner where the torque goal is specified a global goal for density.

7. After the entire step has been completed, the simulation is started and the results will be obtained in a few hours after the COSMOS solver is finished calculating the flow conditions based on our earlier definitions, parameters, and data inputted into the simulation. For higher accuracy result refinement can be done however it will prolonged the simulation progress up to a week therefore no refinement is selected

CHAPTER 4

RESULTS AND DISCUSSION

4.1 INTRODUCTION

In this chapter, the results obtained from both experimentation and simulation will be presented. Several aspect of the result will be shown that is raw data from the experiment and processed data in the form of graph and calculation. The data from the experiment will presented in the form of tabulated data as well as the calculations which led to the values of efficiency which will then will be presented in the form of efficiency curve. The simulation data will also be presented in the same manner with the addition of picture which shows several turbine characteristic which is relevant to our study and explains the flow characteristic within the Francis turbine.

4.2 EXPERIMENT RESULT

From the experiment, data which is relevant to our study was collected and tabulated in an orderly and manage form to provide clear and effective data of presenting the results obtained from the experiment. The justification for these actions are to provide a clear and comprehensive way of presenting the data obtained in both numerical and graphical method which can be interpreted with regards to the fluid flows condition.

Table 4.1: Flow data obtained from experiment

Speed, n (rpm)	Braking force, F (N)	Pressure Head, H (bar)	Torque at shaft, M (Nm)	Power at shaft, P_{ab} (W)	Hyd. Power, P_{hyd} (W)	Efficiency, η
1000	0.0	0.23	0.0000	0.0000	13.4390	0.0000
900	0.3	0.21	0.0075	0.0707	12.2685	0.0576
800	0.5	0.19	0.0125	1.0472	11.1001	0.0943
700	0.8	0.18	0.0200	1.4661	10.5159	0.1394
600	1.1	0.17	0.0275	1.7279	9.9317	0.1740
500	1.3	0.17	0.0325	1.7017	9.9317	0.1713
400	1.5	0.18	0.0375	1.5708	10.5159	0.1494
300	1.7	0.19	0.0425	1.3352	11.1001	0.1203
200	1.9	0.20	0.0475	0.9948	11.6483	0.0851
100	2.2	0.21	0.0550	0.5796	12.2685	0.0472
0	2.5	0.22	0.0625	0.0000	12.8528	0.0000

Source: Experimentation on Francis Turbine

Sample efficiency calculation for 0 rpm

$$M = \frac{F.D}{2} \tag{4.1}$$

$$= \frac{(2.5N).(0.05m)}{2}$$
$$= 0.0625Nm$$

$$P_{ab} = \frac{n.M.2\pi}{60} \tag{4.2}$$

$$= \frac{(0rpm)(0.0625Nm)(2\pi)}{60}$$
$$= 0W$$

$$P_{hyd} = \frac{Q.H.10^5}{1000.60} \tag{4.3}$$

$$= \frac{(35.0530l.min^{-1})(0.22bar)(10^5 Pa.bar^{-1})}{(1000min.m^{-3}).(60\ min.s^{-1})}$$

$$= 12.8528W$$

$$\eta = \frac{P_{ab}}{P_{hyd}} \tag{4.4}$$

$$= \frac{0W}{12.8528W}$$

$$= 0$$
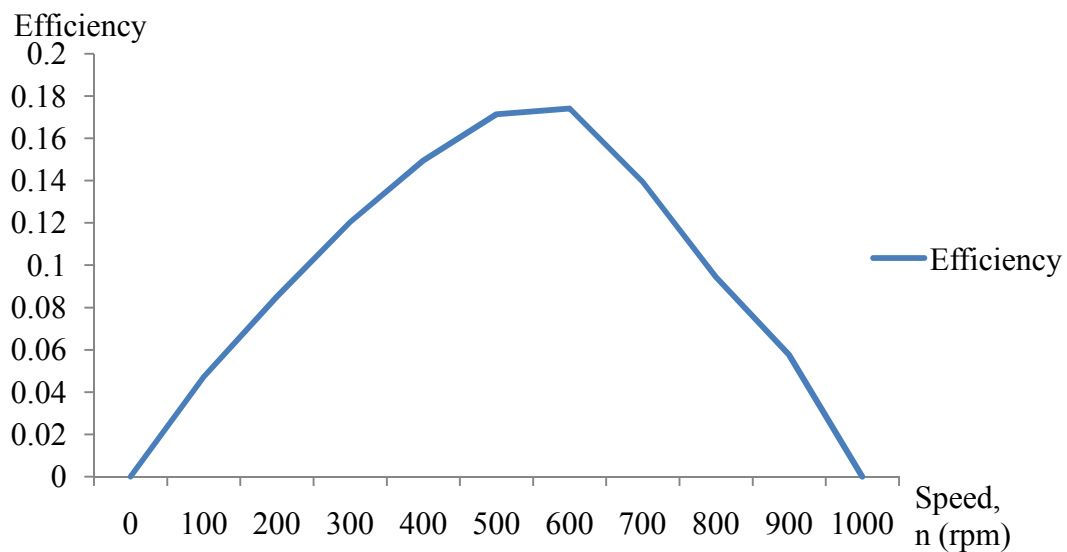
Figure 4.1: Efficiency versus speed graph for experiment data

In Figure 4.1, the data obtained from the experiment are used to calculate the efficiency of the Francis turbine. The efficiency value will then be plotted against the value of the runner speed to obtain the turbine's efficiency curve which will later on be used to validate and verify the results obtained from simulation. The graph curve follows the theoretical shape of efficiency curve suggested for Francis Turbine.

4.3 SIMULATION RESULT

4.3.1 Numerical Results

Using the values of boundary and initial conditions obtained from experiment and during chapter 3, a simulation to imitate the flow condition in a Francis Turbine was done by using COSMOS Flow Simulation

Table 4.2: Flow data obtained from COSMOS simulation for speed range 0-1000rpm

Speed, n (rpm)	Inlet pressure, H (Pa)	Torque at shaft, M (Nm)	Power at shaft, P_{ab} (W)	Hyd. Power, P_{hyd} (W)	Efficiency, η
1000	13826.01	0.054747	5.7330	8.0773	0.7097
900	13812.23	0.059993	5.6542	8.0693	0.7007
800	13808.21	0.065789	5.5115	8.0669	0.6832
700	13819.18	0.072793	5.3360	8.0733	0.6609
600	13826.64	0.077814	4.8891	8.0777	0.6052
500	13831.06	0.079612	4.1684	8.0803	0.5158
400	13846.41	0.079618	3.3350	8.0893	0.4122
300	13853.95	0.083317	2.6174	8.0937	0.3233
200	13863.09	0.088432	1.8521	8.0990	0.2286
100	13871.45	0.091039	0.9533	8.1039	0.1176
0	13895.13	0.090652	0	8.1177	0

Source: COSMOS simulation

Sample efficiency calculation for 0 rpm

$$P_{ab} = \frac{n.M.2\pi}{60} \qquad (4.2)$$

$$= \frac{(0rpm)(0.090652Nm)(2\pi)}{60}$$
$$= 0W$$

A deviation from formula (4.3) by considering pressure in Pa

$$P_{hyd} = \frac{Q.H}{1000.60} \qquad (4.5)$$

$$= \frac{(35.0530 l.min^{-1})(13895.12 Pa)}{(1000 min.m^{-3}).(60\ min.s^{-1})}$$
$$= 8.1177W$$

$$\eta = \frac{P_{ab}}{P_{hyd}} \qquad (4.4)$$

$$= \frac{0W}{8.1177W}$$
$$= 0$$

The efficiency calculation for the simulation will be a little different since the values obtained from simulation will be directly in SI units and several values can be directly obtained from simulation such as the value of torque at shaft which is read from the runner in the simulation assumed to be equal to the torque of shaft which is calculated from the force exerted to the flywheel in the experiment. The base of this assumption is that the diameter of both runner and flywheel is equal whereas the shaft transmitting torque from the runner to the flywheel is lossless.

However, in further discussion, these factors will be used to explain the difference between simulation and experimental data. Note that the speed range for the simulation follows the one obtained from experiment and if analyzed properly, it can be noted that the value of the efficiency increase up to 1000 rpm where as the experiment suggest that upon reaching a certain speed, the value of the efficiency will decrease
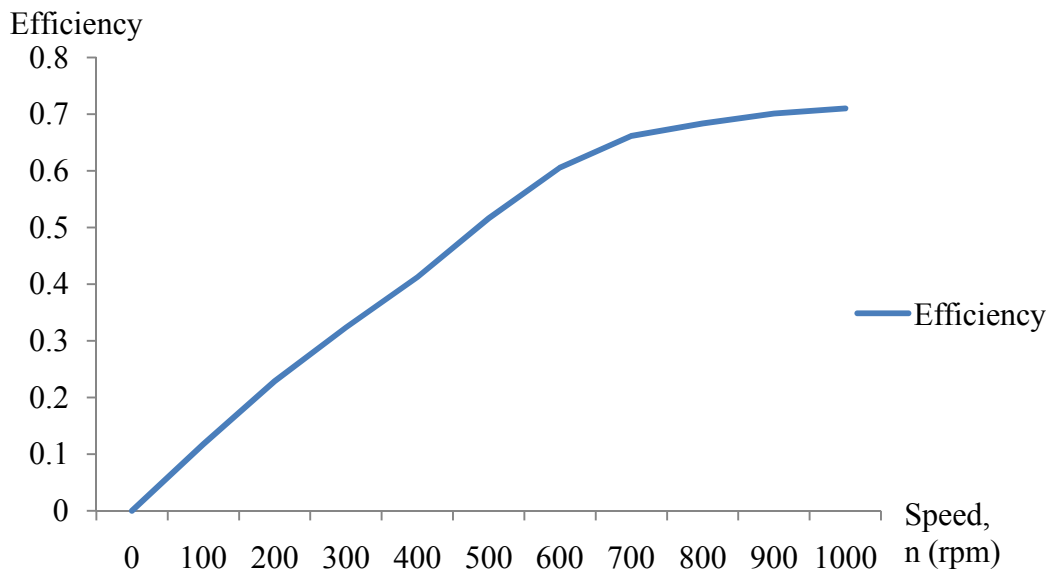
Figure 4.2: Efficiency versus speed graph for simulation data for 0-1000rpm range

The efficiency versus speed curve above only follows the experiment graph up to a certain level where the efficiency is at its peak value for the Francis Turbine. However it can be noted that the increment or the curve of the graph shows a similar pattern to experiment.

Upon further studies and research and reference to the manual provided by the turbine manufacturer, it was highly suggested that the speed operating range of the Gunt Hamburg Demonstration Francis Turbine might actually be higher than those obtained from experiment. Upon realizing this, the simulation is continued by gradually adding the values of the speed by 100 rpm until the reading of the Torque at shaft reaches zero.

Table 4.3: Flow data obtained from COSMOS simulation for speed range 0 - 1700rpm

Speed, n (rpm)	Inlet pressure, H (Pa)	Torque at shaft, M (Nm)	Power at shaft, P_{ab} (W)	Hyd. Power, P_{hyd} (W)	Efficiency, η
1700	13896.22	0	0	8.1184	0
1600	13883.23	0.010564	1.7700	8.1108	0.2182
1500	13877.19	0.021832	3.4293	8.1072	0.4229
1400	13861.59	0.029539	4.3306	8.0981	0.5347
1300	13853.94	0.035679	4.8571	8.0937	0.6001
1200	13846.02	0.043678	5.4875	8.0890	0.6783
1100	13834.74	0.049376	5.6877	8.0824	0.7037
1000	13826.01	0.054747	5.7330	8.0773	0.7097
900	13812.23	0.059993	5.6542	8.0693	0.7007
800	13808.21	0.065789	5.5115	8.0669	0.6832
700	13819.18	0.072793	5.3360	8.0733	0.6609
600	13826.64	0.077814	4.8891	8.0777	0.6052
500	13831.06	0.079612	4.1684	8.0803	0.5158
400	13846.41	0.079618	3.3350	8.0893	0.4122
300	13853.95	0.083317	2.6174	8.0937	0.3233
200	13863.09	0.088432	1.8521	8.0990	0.2286
100	13871.45	0.091039	0.9533	8.1039	0.1176
0	13895.13	0.090652	0	8.1177	0

Source: COSMOS Flow simulation

As observed in the table 4.3, after taking into consideration that the speed operating range for the Francis Turbine is larger than obtained from the experiment, the values of efficiency start to deviate and exhibits similar pattern to those obtained from experiment, the factors contributing to the difference in the values obtained from experiment and simulation will be further explain afterward.

Setting aside the factors affecting, it can be noted that the peak speed of the previous speed range is actually the speed where the efficiency value is at its peak. This led us to
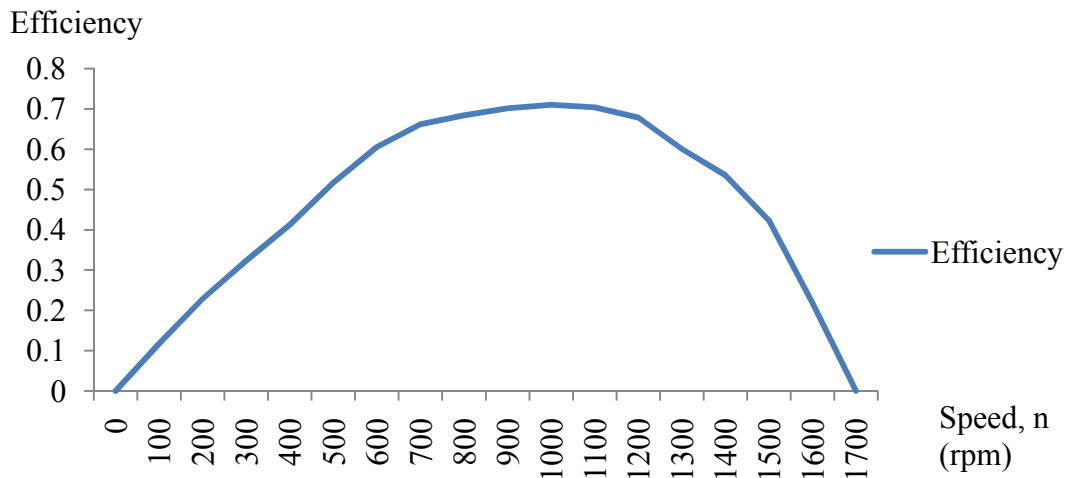
Figure 4.3: Efficiency versus speed graph for simulation data for 0-1700rpm range

The graphical representation of the data displays similar pattern with the experiment data but with less smooth curves yet still displaying consistent pattern. The reasons and discussions of the causes of these results will be discussed later on. From the graph it can be noted that the maximum value of efficiency of the Francis Turbine from the simulation is around 70 percent within the expected range of 60-90 percent of a Francis Turbine. By comparing the efficiency curve of the simulation and cross-referencing the value of maximum efficiency to the efficiency range of a normal Francis Turbine, the results from the simulation was successfully verified and further fluid flow characteristic obtained from the simulation can be used for analysis and interpretation.

4.3.2 Graphical Results

In this part, the graphical results obtained from simulation will be discussed and used to describe the flow characteristic of the turbine by critically analyzing pressure contour and flow of the turbine, velocity contour and flow of the turbine, and the global density in the flow and surface of the turbine.

4.3.2.1 Pressure

4.3.2.1.1 Pressure Flow Trajectories inside Fluid
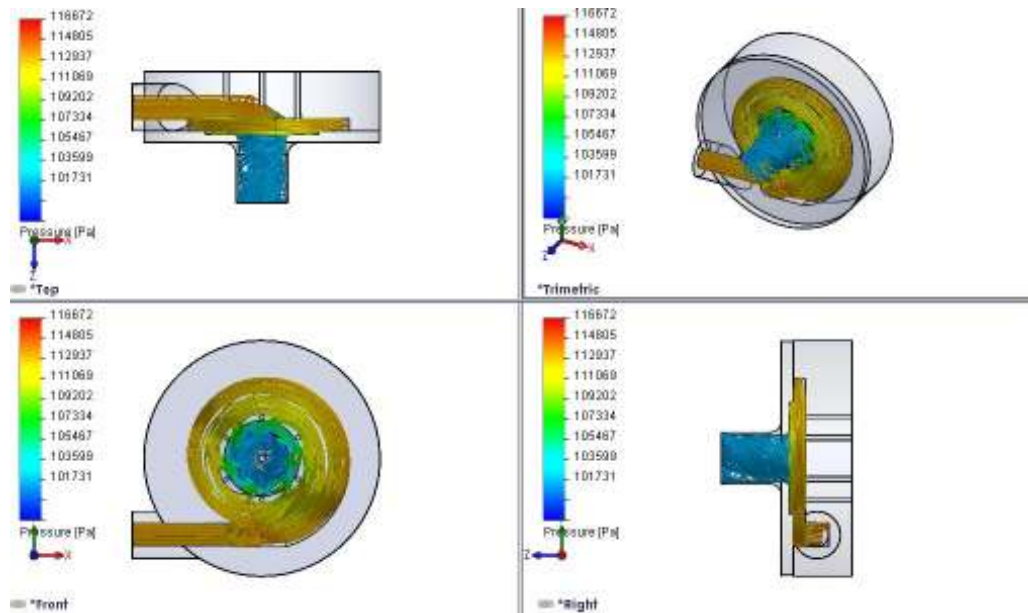
Figure 4.4: Pressure flow inside the fluid in Francis Turbine

As shown in Figure 4.4, the pressure of the fluid (water) inside the turbine is relatively constant with the fluid maintaining a steady pressure up to the fluids entrance through the guiding vanes to the runner. The reason for these is that the high pressure fluid transfers its kinetic energy to the runner as it passes through the runner and losses the energy which reduces the pressure of the fluid after the energy is transferred.

4.3.2.1.2 Pressure Contour on the Internal Surfaces of the Francis Turbine
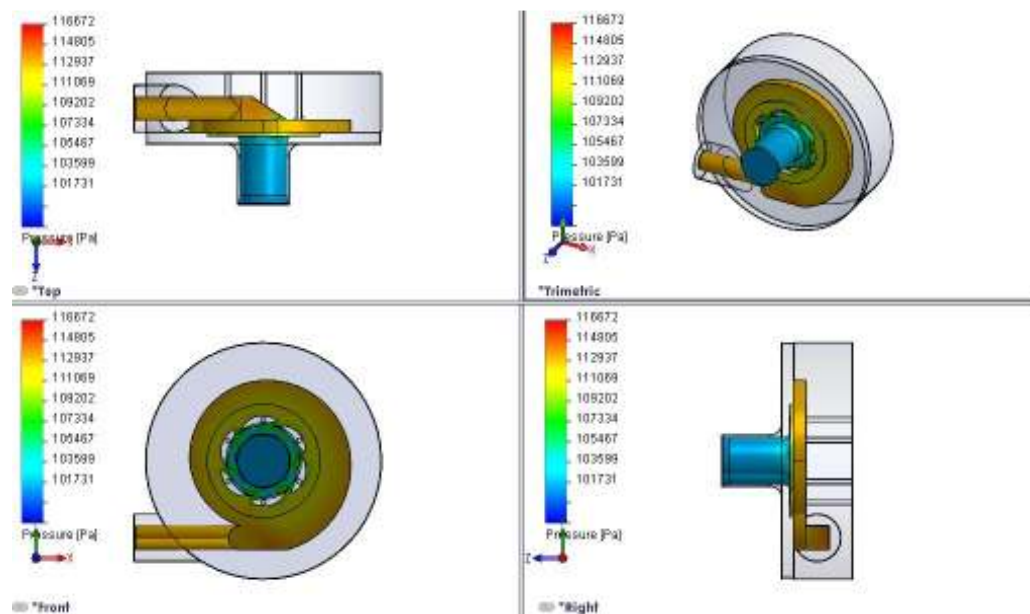
Figure 4.5: Pressure contour on the internal surfaces of the Francis Turbine

In Figure 4.5, it offers us with the pressure reading taken at all internal surfaces in contact with the fluid during simulation and gives us with the reading at all surfaces. With reference to these reading, we are able to make assumptions on how the fluid moves and whether there is part of the turbine which is subjected to extreme pressure and if there is any pressure build-up on the turbine's internal surfaces. If any pressure build-up is spotted, it can be assumed as the turbine's weakest point and the first point which the turbine will fail first. However, as the simulation result shows, the pressure is evenly distributed and the turbine will less likely to fail at any specific location.

By analyzing the pressure distribution on the internal surfaces, it is safe to assume that the fluid flow inside the turbine at the ambient and experiment condition to be turbulent.

4.3.2.1.3 Pressure Contour Cut Plot inside Fluid Flow Region
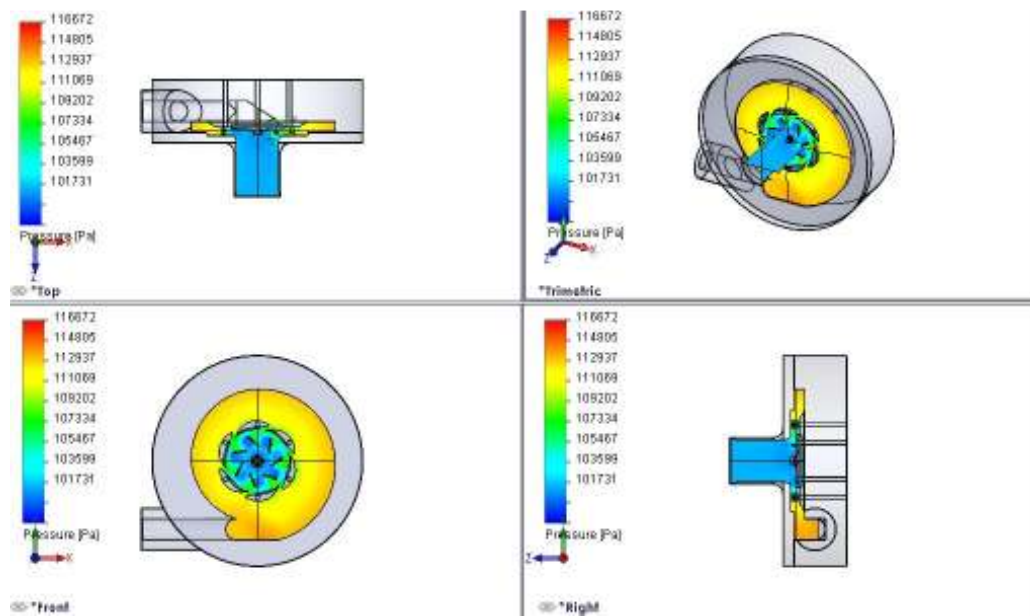
Figure 4.6: Pressure contour cut plot in the fluid flow region

In Figure 4.6, a pressure cut plot of the result is presented where the several cut shown is made parallel to each axis of the model that are the x, y, and z axis. By doing this we will be able to get a more detail view of the pressure distribution inside the turbine. As shown on the front view, our statement on the pressure loss as the energy was transferred to runner is clearly shown by the clear view of a large pressure drop on the turbines runner.

4.3.2.2 Velocity

4.3.2.2.1 Velocity Flow Trajectories inside Fluid
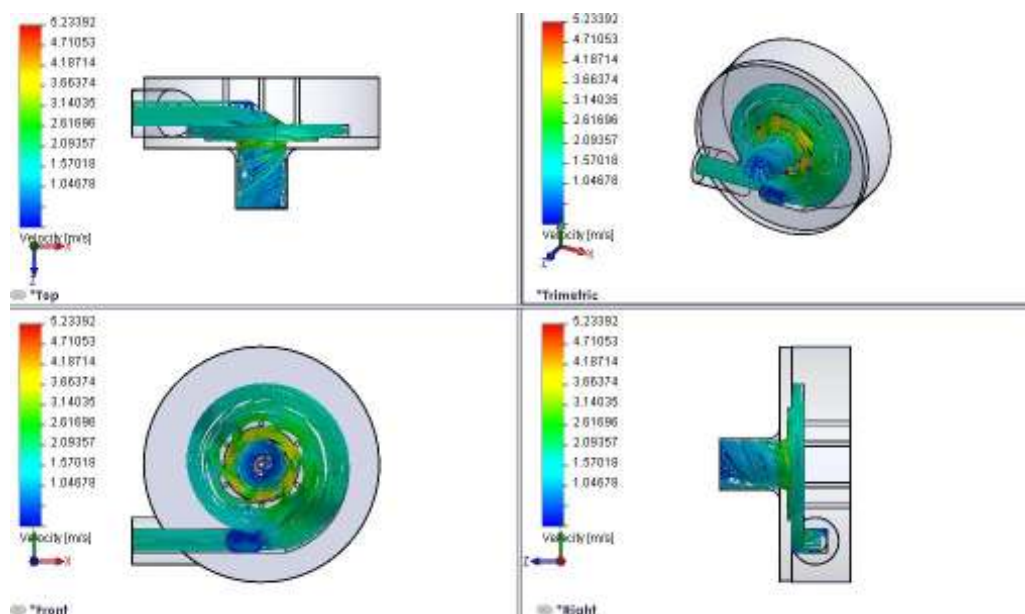
Figure 4.7: Pressure flow inside the fluid in Francis Turbine

In Figure 4.7 the velocity of the fluid flow inside the turbine is shown. It can be noted that velocity is relatively constant but there are several region where the velocity experience change whether increase or decrease. As shown in Figure 4.7, the fluid velocity increases as the fluid passes through the guiding vanes and enters the runner. This can attributed to the movement of the runner as kinetic energy from the moving water is transferred to runner. The fluid speed then decreases as the fluid passes the runner and head through the outlet which due to the runner rotating as the effect of energy transferred to it and not the other way around. However, there is a peculiar pressure drop near the water entrance to the main part of the turbine which yields a warning in COSMOS Flow Simulation signaling that a water vortex has developed inside of the turbine.

4.3.2.2.2 Velocity Contour on Turbine Internal Surfaces
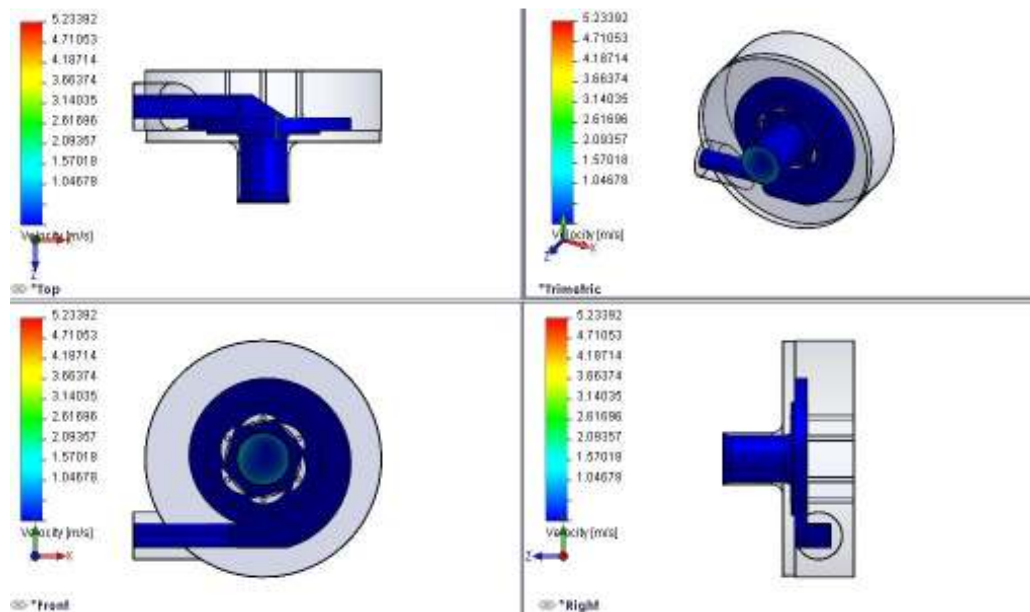
Figure 4.8: Velocity contour on the internal surfaces of the Francis Turbine

In Figure 4.8, the fluid velocity on the turbine internal surfaces are shown to investigate the fluid characteristic around the internal surfaces of the turbine. In the Figure 4.8, it is clearly shown that fluid flow on the internal surfaces of the turbine in constant with nearly no change what so ever in the velocity except for the slight increase at the outlet of the turbine. The vortex that exist earlier in the velocity fluid flow doesn't show any difference in the internal surface contour since the vortex that occurred has relatively the lowest velocity in the velocity fluid flow in Figure 4.7. The constant velocity contour furthermore confirms the earlier statement of the fluid flow being turbulent throughout the entire turbine as discussed in chapter 2.

4.3.2.2.3 Velocity Contour Cut Plot inside Fluid Flow Region
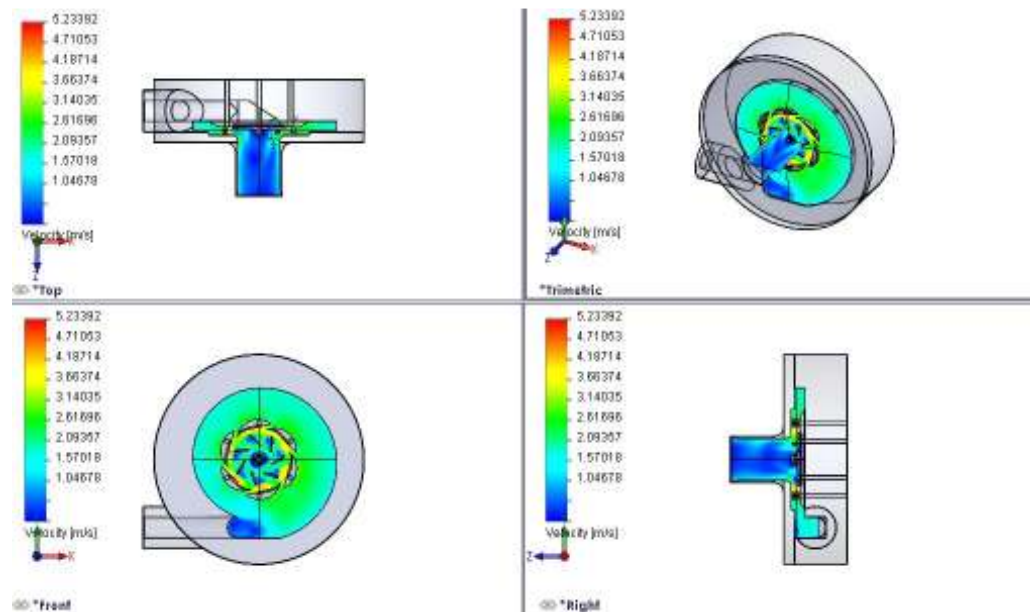
Figure 4.9: Velocity contour cut plot in the fluid flow region

The velocity contour cut plot inside fluid flow region shown in Figure 4.9 gives a clearer view of the fluid velocity in the fluid flow region of the turbine during operating condition. The figure shows that the velocity major increase is at the runner as shown in Figure 4.7 but there is also a slight increase as the fluid hits the wall of the turbine and moves to the runner of the turbine, the increase in fluid velocity is attributed to the molecular energy of water as the water particles collide with each other and the turbine wall.

This provides additional energy to the moving water in the sense of velocity increment. However due to the small energy gained as the result of these collisions, the increase in the fluid velocity is not really noticeable. In Figure 4.9, it is clearly shown that the vortex results in velocity drop in the main turbine compartment, however it is not known whether the presence of the vortex has any sort of huge effect on the fluid flow characteristic within the Francis Turbine.

4.3.2.3 Density

4.3.2.3.1 Density flow Trajectories inside fluid
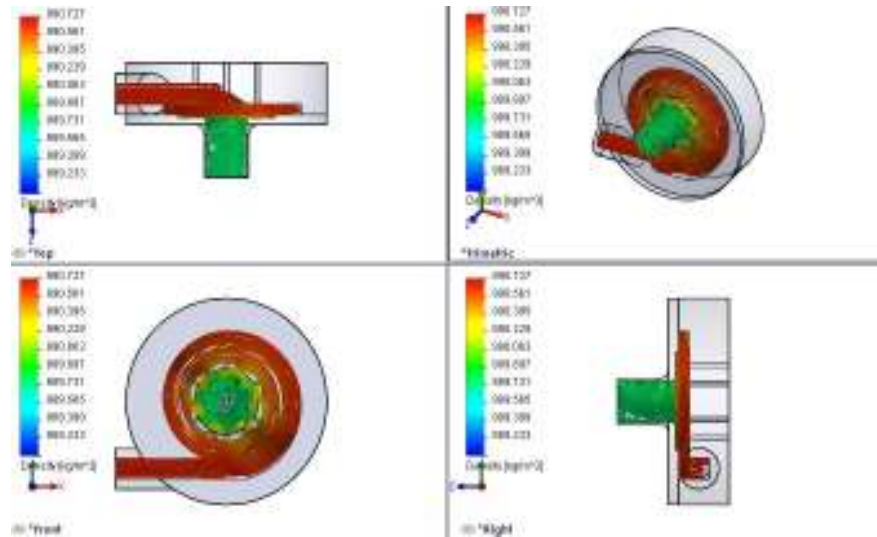
Figure 4.10: Density flow inside the fluid in Francis Turbine

4.3.2.3.2 Density Contour on Turbine Internal Surfaces
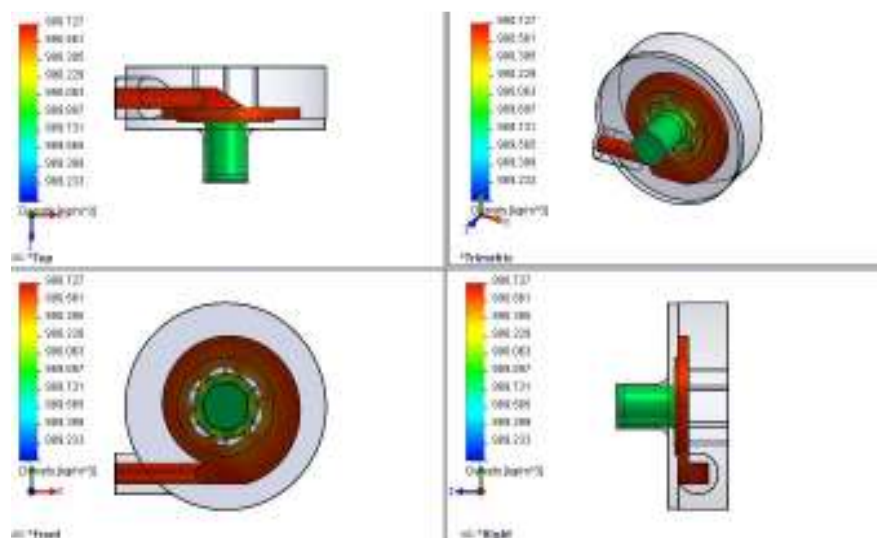
Figure 4.11: Density contour on the internal surfaces of the Francis Turbine

Both Figure 4.10 and 4.11 are used to evaluate whether cavitations occurs in the turbine. To identify if cavitations occurs, the result is analyzed to see whether there is any sudden density drop in the turbine. During cavitations occurrence, bubbles filled with air forms around the guiding vanes and runner which result in runner and guiding vanes cracking. By identifying if there is density drop up to the density of air cavitations can be identified. However based on both Figure 4.10 and 4.11 there is no density drop to air density level which makes it safe to assume that cavitations doesn't occur in the simulation.

4.4 VALIDATION

The validation study as mention earlier is done by mean of comparing efficiency curve pattern. As shown in Figure 4.12, both line exhibits similar pattern but with different graph curve. Since the pattern is similar, the results are considered validated and reason of the values differences will be discussed on next sub-chapter.
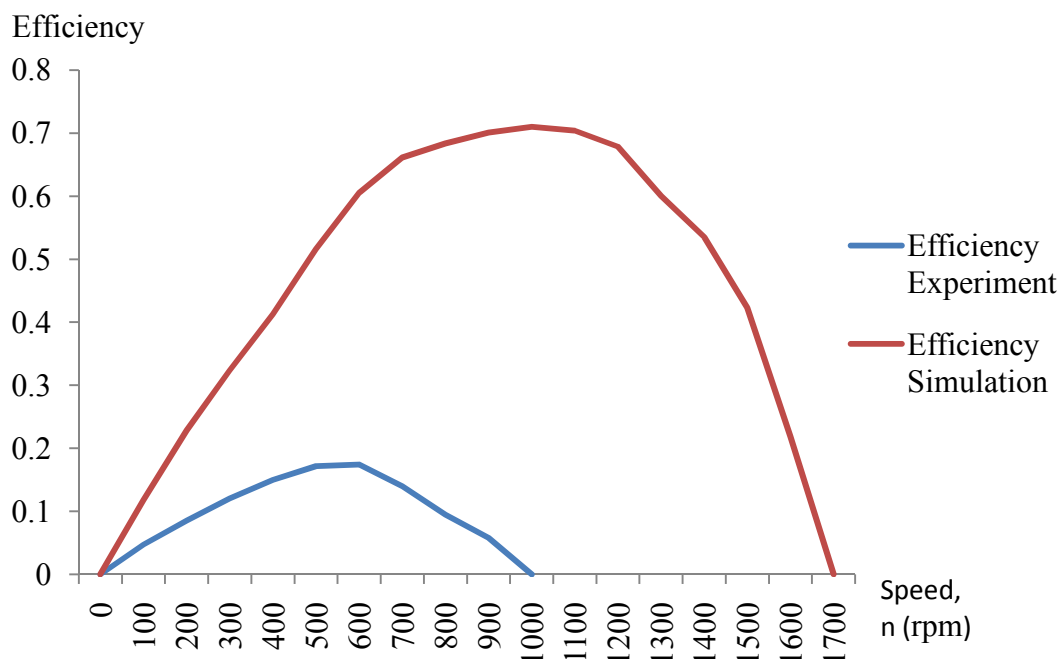
Figure 4.12: Efficiency versus speed graph for experiment and simulation data

$$\% = \frac{\eta_{\,simulation} - \eta_{\,experiment}}{\eta_{\,simulation}} \tag{4.5}$$

$$= \frac{0.7097 - 0.1740}{0.7097}$$
$$= 0.7548 \ @ \ 75.48\%$$

Note that only the maximum value of efficiency is considered when determining the percentage in the efficiency difference between simulation and experiment since the speed operating range for the experiment and simulation is different.

4.5 DISCUSSION

As observed from table 4.1 and Figure 4.1, the efficiency value for the Gunt Hamburg Demonstration Francis Turbine obtained from experiment is rated at a mere 17 percent efficiency, a far cry from the theoretical value of 60 – 90 percent. There are several possible factors contributing these low efficiency values that was observed during experiment was the physical condition of the turbine itself.
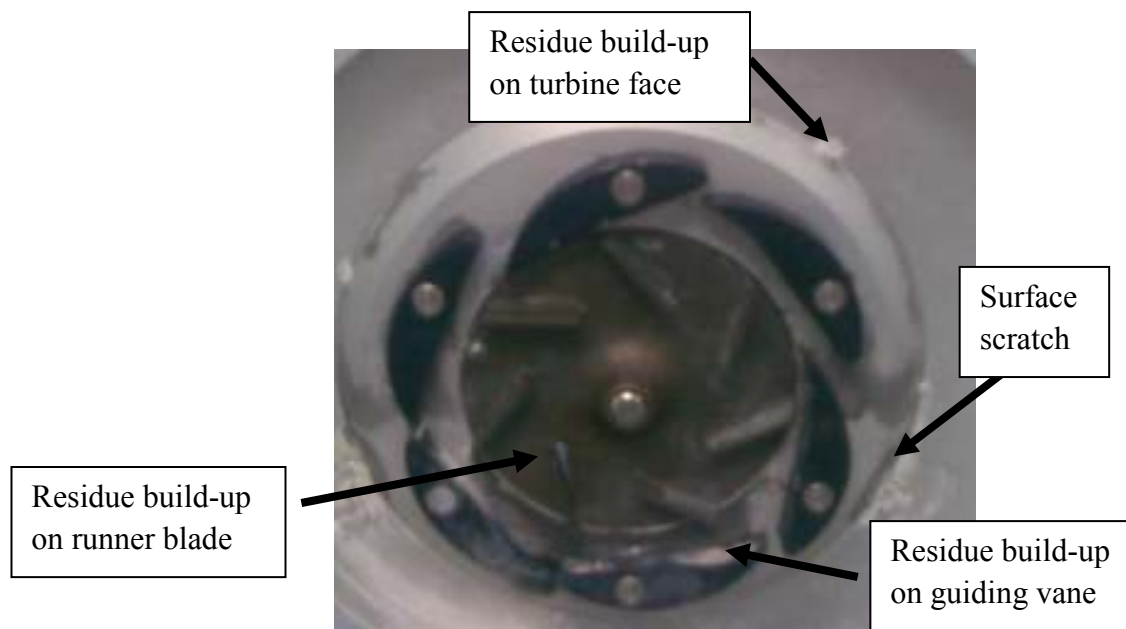
Figure 4.13: Foreign build-up on turbine face

49

Dent on one
of the
guiding vane

Figure 4.13: Dent and scratches on guiding vanes

One of the
guiding
vane tips is
broken
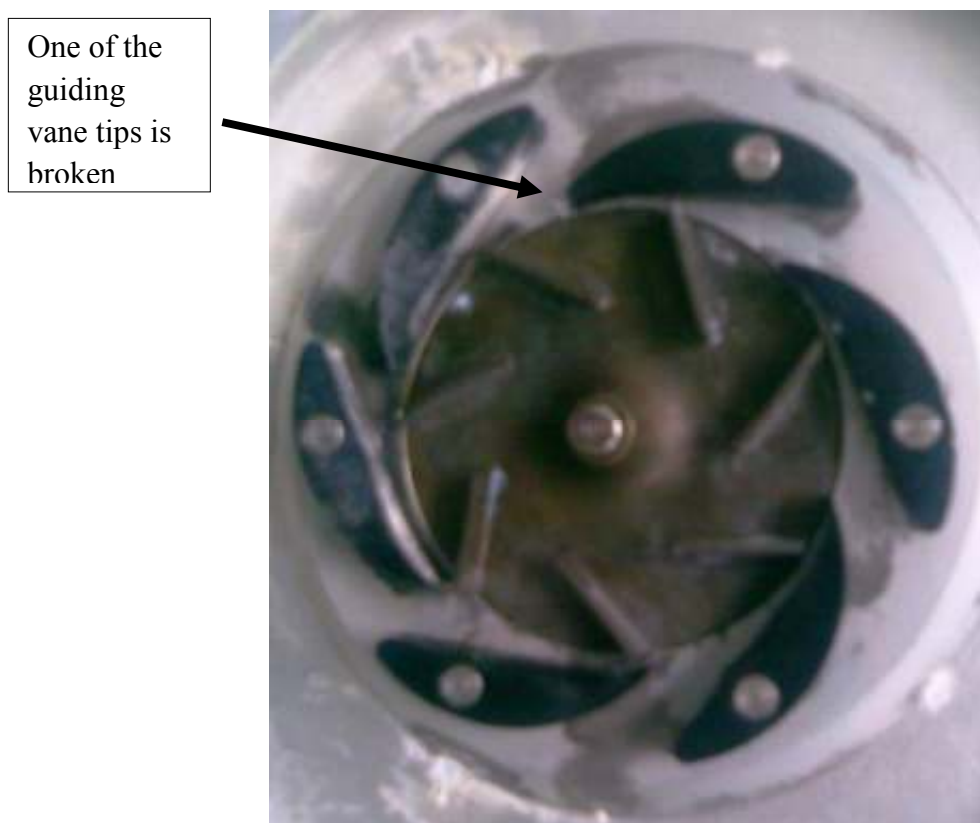
Figure 4.14: Guiding vanes disorientations

The Figure 4.12, 4.13, and 4.14 shows the physical imperfection and damage to the physique of the turbine. The arrows in Figure 4.12 points out to the foreign build-up of plaque caused from continuous usage of unclean water as the operating fluid. As pointed out by the arrows, the build-up center around the turbine's guiding vanes and runner which are the most critical part of the turbine. The formation of these build-up attribute to the loss of energy due to the friction between the flowing water with these build-up.

In the next figure that is Figure 4.13 shows the presence of dent on the guiding vanes which will lead to the flow being diverted from its original direction and colliding with the movement of other flow trajectories. By diverting the flow trajectories of the flowing water, the total energy of the water that is transferred to the runner is reduced. During the pre-experimental process, these plaque build-up and dent were tried to be fixed by means of cleaning the plaque and patching the dent, however, after a few unsuccessful trial it was obvious that the physical imperfection cannot be corrected without further damaging the turbine and making matters worse. After a brief research it was concluded that these physical imperfection will indeed affect the reading but not the efficiency curve which is the most critical data to be obtained from the experiment for validation purposes.

Next in Figure 4.14, the figure displays the disorientations of the guiding vanes with the vanes pointed by the arrow having the curvature tip broken. During pre-experimental process, we have tried to align the guiding vanes back to the original and correct vanes position but were failed by the aging components of the turbine which limits the amount of vanes correction done. To overcome this, the Turbine was left to run and the vane angle was adjusted until the cavitations are decreased to the lowest possible. The angle is the taken as the average angle of all vane angles.

In the simulation, using the speed range obtained from the experiment we were not able to obtain the same efficiency curve as those obtained from experiment. This is attributed to the turbine age. The shaft which transfer torque from the runner to the flywheel has undergone numerous experimentation process which led to the wear and tear of the part. Furthermore, the continuous usage suggest that the increase in the

surface roughness on the shaft and the contacting surface. Including these factors in the assumption, it can be estimated that the energy transferred to the flywheel is lost at the shaft resulting in the decrease in operating speed range since energy is lost from the runner during transfer process.

In the simulation, the maximum value of efficiency rated is around 70 percent where as the theoretical efficiency value is around 90 percent. The reason for this is that the theoretical is the estimated efficiency value for the normal conventional Francis Turbines used in dam where the energy obtained from the is obtained from both radial and axial flow where as the Francis Turbine of interest only gain energy from axial flow. This alone explains the reason why the efficiency of the simulation only reaches 70 percent.

In the simulation, due to the geometric design of the Francis Turbine a water vortex gathers at the inlet of the main body of the Francis Turbine. The fluid at this region seems to have similar pressure to the surrounding fluid but sport and obvious drop in velocity. This phenomenon may at first seem to affect the reading of the turbine but upon closer inspection at Figure 4.9 it can noticed that the vortex region does not restrict flow as it only gather at the front part of the water entrance.

CHAPTER 5

CONCLUSION AND RECOMMENDATION

5.1 INTRODUCTION

This chapter will conclude the previous chapters and provide a short summary of previously stated item and discussed issue regarding to the project. In this chapter we will try to make a conclusion on the result obtained from simulation and experiment as well as try to provide a brief summary on how the project has been able to meet the goal and objective and justify the project done.

5.2 CONCLUSION

At the beginning of this paper, several objectives were made to ensure that the project had a clear set of goals to achieve which will avoid the project to be strayed and led in the wrong directions. To further guide the project specific scopes was also pre-determined which will focus the efforts into a channeled direction. The scope includes CAD solid modeling, CFD analysis, turbine parameter modification, turbine efficiency improvement, validation study of efficiency and flow characteristic. After the project was finish it can be concluded that it was successful as the objectives initially set was achieved while following the scopes set.

The first objective was create a complete, accurate and working 3D model of UMP's Gunt Hamburg Francis Turbine in CAD was successful where by using the dimensions of the actual Francis Turbine, a CAD model was successfully modeled with regards to the operational part of the turbine. The second objective was to subject the constructed 3D model of UMP's Francis Turbine to boundary and initial condition such as the working environment of a Francis Turbine so that the fluid flow can be analyzed by a CFD code was also successfully completed by using the boundary and initial

condition obtain during experiment and these condition are set at the relevant part of the turbine CAD modeling and goals are set at region relevant to obtain needed data.

For the third and last objective of studying the flow characteristic of a Francis Turbine by means of analyzing the simulation result and interpreting them into their respective characteristic was completed by analyzing the graphical results of relevant parameters of Francis Turbine such as pressure, velocity, and density and interpretation based on the results are made to predict the flow characteristic. Based on the data obtained from the entire experiment it was discovered that the simulation efficiency value obtained is around 75 percent higher than experiment attributed to the physical imperfections on the Francis Turbine and the conditions of the available apparatus at the time of experiment.

Considering all of the objectives are successfully achieve by utilizing the entire pre-set objective, it can be concluded that this project was a success and several interesting find was encountered like the vortex formation on the turbine body entrance. The project is deemed necessary as it contribute a complete flow characteristic inside UMP's Gunt Hamburg Francis Turbine where as previous research only considered critical parts such as the runner and guiding vanes.

5.2 RECOMMENDATION

For future studies it is suggested that the simulation be done in a smaller mesh size to get more accurate and reliable data. The simulation was done in level 4 meshes without refinement due to the amount of time taken if the simulation was done in higher mesh level and refinement. In future studies the variables on the turbine study can also be increase by adding variable surface roughness, flow rate and perhaps modify the physical aspect of the turbine such as runner blade number and guiding vanes number. For further accurate data, it is suggested that future study uses advance flow simulation software such as ANSYS CFX.

REFERENCES

[1] Qian Z. D., Yang J. D., Huai W. X. 2006. Numerical simulation and analysis of pressure pulsation in Francis Hydraulic Turbine with air admission.

[2] Xiao R., Wang Z. W., Luo Y. Y. 2008. Dynamic Stresses in a Francis Turbine Runner Based on Fluid-Structure Interaction Analysis.

[3] Ruixia Q. 2008. Flow Field Measurements in a distributor of a Francis Turbine.

[4] Zhang L. X., Wang W. Q . 2006. Intrinsic features of turbulent flow in strongly 3-D skew blade passage of a Francis Turbine.

[5] Marjavaara, B. D. 2004. CFD Driven Optimization of Hydraulic Turbine Draft Tubes using Surrogate Models.

[6] Eerle, P., Couston, M. and Sabourin, M. 2002. Refurbishment of low head Francis Turbines, Proceedings of the XXIst IAHR Symposium on Hydraulic Machinery and Systems (ed. F. Avellan, G. Ciocan and S. Kvicinsky) IAHR, Lausanne.

[7] Avellan, F. 2000 Flow Investigation in a Francis Draft Tube: the FLINDT Project, Proceedings of 20th IAHR Symposium on Hydraulic Machinery and System.

[8] Marjavaara, B. D. 2004. Parameterization and Flow Design Optimization of Hydraulic Turbine Draft Tubes, Licentiate Thesis, Luleå University of Technology.

[9] Guo P. C., Luo X. Q., Zheng X. B. et al. 2006. Numerical investigation of three-dimension turbulent flow fields in a Francis turbine.

[10] Shao Q., Liu S. H., Wu Y. L. et al. 2004. Three-dimensional simulation of unsteady flow in model Francis hydraulic turbine.

[11] Zhang K. W. et al. 2005. Study on PIV measurement of exit velocity distribution of Francis turbine runner.

[12] Mufeed O. 1999. A Summary of Environmentally Friendly Turbine Design Concepts.

[13] Teodor M., Romeo S. R., Alexandru B., Sebastian M., Sandor B. 2006. Development of francis turbine model with swirling flow control.

APPENDIX A

Full experiment calculation

For 0 rpm

$$M = \frac{F.D}{2}$$

$$= \frac{(2.5N).(0.05m)}{2}$$
$$= 0.0625Nm$$

$$P_{ab} = \frac{n.M.2\pi}{60}$$

$$= \frac{(0rpm)(0.0625Nm)(2\pi)}{60min.sec^{-1}}$$
$$= 0W$$

$$P_{hyd} = \frac{Q.H.10^5}{1000.60}$$

$$= \frac{(35.0530l.min^{-1})(0.22bar)(10^5Pa.bar^{-1})}{(1000min.m^{-3}).(60\ min.s^{-1})}$$
$$= 12.8528W$$

$$\eta = \frac{P_{ab}}{P_{hyd}}$$

$$= \frac{0W}{12.8528W}$$
$$= 0$$

For 100 rpm

$$M = \frac{F.D}{2}$$

$$= \frac{(2.2N).(0.05m)}{2}$$
$$= 0.0550 Nm$$

$$P_{ab} = \frac{n.M.2\pi}{60}$$

$$= \frac{(100rpm)(0.0550Nm)(2\pi)}{60min.sec^{-1}}$$
$$= 0.5796W$$

$$P_{hyd} = \frac{Q.H.10^5}{1000.60}$$

$$= \frac{(35.0530l.min^{-1})(0.21bar)(10^5Pa.bar^{-1})}{(1000min.m^{-3}).(60\ min.s^{-1})}$$
$$= 12.2685W$$

$$\eta = \frac{P_{ab}}{P_{hyd}}$$

$$= \frac{0.5796W}{12.2685W}$$
$$= 0.0472$$

For 200 rpm

$$M = \frac{F.D}{2}$$

$$= \frac{(1.9N).(0.05m)}{2}$$

$$= 0.0475 Nm$$

$$P_{ab} = \frac{n.M.2\pi}{60}$$

$$= \frac{(200rpm)(0.0475Nm)(2\pi)}{60 min.sec^{-1}}$$

$$= 0.9948W$$

$$P_{hyd} = \frac{Q.H.10^5}{1000.60}$$

$$= \frac{(35.0530 l.min^{-1})(0.20 bar)(10^5 Pa.bar^{-1})}{(1000 min.m^{-3}).(60\ min.s^{-1})}$$

$$= 11.6483W$$

$$\eta = \frac{P_{ab}}{P_{hyd}}$$

$$= \frac{0.9948W}{11.6483W}$$

$$= 0.0851$$

For 300 rpm

$$M = \frac{F.D}{2}$$

$$= \frac{(1.7N).(0.05m)}{2}$$

$$= 0.0375 Nm$$

$$P_{ab} = \frac{n.M.2\pi}{60}$$

$$= \frac{(300rpm)(0.0375Nm)(2\pi)}{60min.\,sec^{-1}}$$

$$= 1.3352W$$

$$P_{hyd} = \frac{Q.H.10^5}{1000.60}$$

$$= \frac{(35.0530l.\,min^{-1})(0.19bar)(10^5Pa.\,bar^{-1})}{(1000min.\,m^{-3}).(60\,min.\,s^{-1})}$$

$$= 11.1001W$$

$$\eta = \frac{P_{ab}}{P_{hyd}}$$

$$= \frac{1.3352W}{11.1001W}$$

$$= 0.1203$$

For 400 rpm

$$M = \frac{F.D}{2}$$

$$= \frac{(1.5N).(0.05m)}{2}$$

$$= 0.0375Nm$$

$$P_{ab} = \frac{n.M.2\pi}{60}$$

$$= \frac{(400rpm)(0.03755Nm)(2\pi)}{60min.\,sec^{-1}}$$

$$= 1.5708W$$

$$P_{hyd} = \frac{Q.H.10^5}{1000.60}$$

$$= \frac{(35.0530 l. \, min^{-1})(0.18 bar)(10^5 Pa. \, bar^{-1})}{(1000 min. \, m^{-3}). \, (60 \, min. \, s^{-1})}$$

$$= 10.5159 W$$

$$\eta = \frac{P_{ab}}{P_{hyd}}$$

$$= \frac{1.5708 W}{10.5159 W}$$

$$= 0.1494$$

For 500 rpm

$$M = \frac{F.D}{2}$$

$$= \frac{(1.3N). \, (0.05m)}{2}$$

$$= 0.0325 Nm$$

$$P_{ab} = \frac{n. \, M. \, 2\pi}{60}$$

$$= \frac{(500 rpm)(0.0325 Nm)(2\pi)}{60 min. \, sec^{-1}}$$

$$= 1.7017 W$$

$$P_{hyd} = \frac{Q.H.10^5}{1000.60}$$

$$= \frac{(35.0530 l. \, min^{-1})(0.17 bar)(10^5 Pa. \, bar^{-1})}{(1000 min. \, m^{-3}). \, (60 \, min. \, s^{-1})}$$

$$= 9.9317 W$$

$$\eta = \frac{P_{ab}}{P_{hyd}}$$

$$= \frac{1.7017W}{9.9317W}$$

$$= 0.1713$$

For 600 rpm

$$M = \frac{F.D}{2}$$

$$= \frac{(1.1N).(0.05m)}{2}$$

$$= 0.0275Nm$$

$$P_{ab} = \frac{n.M.2\pi}{60}$$

$$= \frac{(600rpm)(0.0275Nm)(2\pi)}{60min.sec^{-1}}$$

$$= 1.7279W$$

$$P_{hyd} = \frac{Q.H.10^5}{1000.60}$$

$$= \frac{(35.0530l.min^{-1})(0.17bar)(10^5Pa.bar^{-1})}{(1000min.m^{-3}).(60\ min.s^{-1})}$$

$$= 9.9317W$$

$$\eta = \frac{P_{ab}}{P_{hyd}}$$

$$= \frac{1.7279W}{9.9317W}$$

$$= 0.1740$$

For 700 rpm

$$M = \frac{F.D}{2}$$

$$= \frac{(0.8N).(0.05m)}{2}$$
$$= 0.0200Nm$$

$$P_{ab} = \frac{n.M.2\pi}{60}$$

$$= \frac{(700rpm)(0.0200Nm)(2\pi)}{60min.sec^{-1}}$$
$$= 1.4661W$$

$$P_{hyd} = \frac{Q.H.10^5}{1000.60}$$

$$= \frac{(35.0530l.min^{-1})(0.18bar)(10^5Pa.bar^{-1})}{(1000min.m^{-3}).(60\ min.s^{-1})}$$
$$= 10.5159W$$

$$\eta = \frac{P_{ab}}{P_{hyd}}$$

$$= \frac{1.4661W}{10.5159W}$$
$$= 0.1394$$

For 800 rpm

$$M = \frac{F.D}{2}$$

$$= \frac{(0.5N).(0.05m)}{2}$$

$$= 0.0125 Nm$$

$$P_{ab} = \frac{n.M.2\pi}{60}$$

$$= \frac{(800rpm)(0.0125Nm)(2\pi)}{60min.sec^{-1}}$$

$$= 1.0472W$$

$$P_{hyd} = \frac{Q.H.10^5}{1000.60}$$

$$= \frac{(35.0530l.min^{-1})(0.19bar)(10^5Pa.bar^{-1})}{(1000min.m^{-3}).(60\ min.s^{-1})}$$

$$= 11.1001W$$

$$\eta = \frac{P_{ab}}{P_{hyd}}$$

$$= \frac{1.0472W}{11.1001W}$$

$$= 0.0943$$

For 900 rpm

$$M = \frac{F.D}{2}$$

$$= \frac{(0.3N).(0.05m)}{2}$$

$$= 0.0075 Nm$$

$$P_{ab} = \frac{n.M.2\pi}{60}$$

$$= \frac{(900 rpm)(0.0075 Nm)(2\pi)}{60 min. sec^{-1}}$$

$$= 0.0707W$$

$$P_{hyd} = \frac{Q.H.10^5}{1000.60}$$

$$= \frac{(35.0530 l. min^{-1})(0.21 bar)(10^5 Pa. bar^{-1})}{(1000 min. m^{-3}).(60\ min. s^{-1})}$$

$$= 12.2685W$$

$$\eta = \frac{P_{ab}}{P_{hyd}}$$

$$= \frac{0.0707W}{12.2685W}$$

$$= 0.0576$$

For 1000 rpm

$$M = \frac{F.D}{2}$$

$$= \frac{(0.0N).(0.05m)}{2}$$

$$= 0Nm$$

$$P_{ab} = \frac{n.M.2\pi}{60}$$

$$= \frac{(1000 rpm)(0 Nm)(2\pi)}{60 min. sec^{-1}}$$

$$= 0W$$

$$P_{hyd} = \frac{Q.H.10^5}{1000.60}$$

$$= \frac{(35.0530l.min^{-1})(0.23bar)(10^5Pa.bar^{-1})}{(1000min.m^{-3}).(60\ min.s^{-1})}$$

$$= 13.4390W$$

$$\eta = \frac{P_{ab}}{P_{hyd}}$$

$$= \frac{0W}{13.4390W}$$

$$= 0$$

Complete calculation for simulation result

For 0 rpm

$$P_{ab} = \frac{n.M.2\pi}{60}$$

$$= \frac{(0rpm)(0.090652Nm)(2\pi)}{60min.sec^{-1}}$$

$$= 0W$$

$$P_{hyd} = \frac{Q.H}{1000.60}$$

$$= \frac{(35.0530l.min^{-1})(13895.12Pa)}{(1000min.m^{-3}).(60\ min.s^{-1})}$$

$$= 8.1177W$$

$$\eta = \frac{P_{ab}}{P_{hyd}}$$

$$= \frac{0W}{8.1177W}$$

$$= 0$$

For 100 rpm

$$P_{ab} = \frac{n.M.2\pi}{60}$$

$$= \frac{(100rpm)(0.091039Nm)(2\pi)}{60min.sec^{-1}}$$

$$= 0.9533W$$

$$P_{hyd} = \frac{Q.H}{1000.60}$$

$$= \frac{(35.0530l.min^{-1})(13871.45Pa)}{(1000min.m^{-3}).(60\ min.s^{-1})}$$

$$= 8.1039W$$

$$\eta = \frac{P_{ab}}{P_{hyd}}$$

$$= \frac{0.9533W}{8.1039W}$$

$$= 0.1176$$

For 200 rpm

$$P_{ab} = \frac{n.M.2\pi}{60}$$

$$= \frac{(200rpm)(0.088432Nm)(2\pi)}{60min.sec^{-1}}$$

$$= 1.8521W$$

$$P_{hyd} = \frac{Q.H}{1000.60}$$

$$= \frac{(35.0530 l.min^{-1})(13863.09 Pa)}{(1000 min.m^{-3}).(60\ min.s^{-1})}$$

$$= 8.0990\text{W}$$

$$\eta = \frac{P_{ab}}{P_{hyd}}$$

$$= \frac{1.8521 W}{8.0990 W}$$

$$= 0.2286$$

For 300 rpm

$$P_{ab} = \frac{n.M.2\pi}{60}$$

$$= \frac{(300 rpm)(0.083317 Nm)(2\pi)}{60 min.sec^{-1}}$$

$$= 2.6174 W$$

$$P_{hyd} = \frac{Q.H}{1000.60}$$

$$= \frac{(35.0530 l.min^{-1})(13853.95 Pa)}{(1000 min.m^{-3}).(60\ min.s^{-1})}$$

$$= 8.0937\text{W}$$

$$\eta = \frac{P_{ab}}{P_{hyd}}$$

$$= \frac{2.6174 W}{8.0937 W}$$

$$= 0.3233$$

For 400 rpm

$$P_{ab} = \frac{n.M.2\pi}{60}$$

$$= \frac{(400rpm)(0.079618Nm)(2\pi)}{60min.sec^{-1}}$$
$$= 3.3350W$$

$$P_{hyd} = \frac{Q.H}{1000.60}$$

$$= \frac{(35.0530l.min^{-1})(13846.41Pa)}{(1000min.m^{-3}).(60\ min.s^{-1})}$$
$$= 8.0893W$$

$$\eta = \frac{P_{ab}}{P_{hyd}}$$

$$= \frac{3.3350W}{8.0893W}$$
$$= 0.4122$$

For 500 rpm

$$P_{ab} = \frac{n.M.2\pi}{60}$$

$$= \frac{(500rpm)(0.079612Nm)(2\pi)}{60min.sec^{-1}}$$
$$= 4.1684W$$

$$P_{hyd} = \frac{Q.H}{1000.60}$$

$$= \frac{(35.0530l.\,min^{-1})(13831.06Pa)}{(1000min.\,m^{-3}).(60\,min.\,s^{-1})}$$

$$= 8.0803W$$

$$\eta = \frac{P_{ab}}{P_{hyd}}$$

$$= \frac{4.1684W}{8.0803W}$$

$$= 0.5158$$

For 600 rpm

$$P_{ab} = \frac{n.\,M.\,2\pi}{60}$$

$$= \frac{(600rpm)(0.077814Nm)(2\pi)}{60min.\,sec^{-1}}$$

$$= 4.8891W$$

$$P_{hyd} = \frac{Q.\,H}{1000.60}$$

$$= \frac{(35.0530l.\,min^{-1})(13826.64Pa)}{(1000min.\,m^{-3}).(60\,min.\,s^{-1})}$$

$$= 8.0777W$$

$$\eta = \frac{P_{ab}}{P_{hyd}}$$

$$= \frac{4.8891W}{8.0777W}$$

$$= 0.6052$$

For 700 rpm

$$P_{ab} = \frac{n.M.2\pi}{60}$$

$$= \frac{(700rpm)(0.072793Nm)(2\pi)}{60min.sec^{-1}}$$

$$= 5.3360W$$

$$P_{hyd} = \frac{Q.H}{1000.60}$$

$$= \frac{(35.0530l.min^{-1})(13819.18Pa)}{(1000min.m^{-3}).(60\ min.s^{-1})}$$

$$= 8.0733W$$

$$\eta = \frac{P_{ab}}{P_{hyd}}$$

$$= \frac{5.3360W}{8.0733W}$$

$$= 0.6609$$

For 800 rpm

$$P_{ab} = \frac{n.M.2\pi}{60}$$

$$= \frac{(800rpm)(0.065789Nm)(2\pi)}{60min.sec^{-1}}$$

$$= 5.5115W$$

$$P_{hyd} = \frac{Q.H}{1000.60}$$

$$= \frac{(35.0530 l.\,min^{-1})(13808.21 Pa)}{(1000 min.\,m^{-3}).(60\ min.\,s^{-1})}$$

$$= 8.0669 W$$

$$\eta = \frac{P_{ab}}{P_{hyd}}$$

$$= \frac{5.5115 W}{8.0669 W}$$

$$= 0.6832$$

For 900 rpm

$$P_{ab} = \frac{n.M.2\pi}{60}$$

$$= \frac{(900 rpm)(0.059993 Nm)(2\pi)}{60 min.\,sec^{-1}}$$

$$= 5.6542 W$$

$$P_{hyd} = \frac{Q.H}{1000.60}$$

$$= \frac{(35.0530 l.\,min^{-1})(13812.23 Pa)}{(1000 min.\,m^{-3}).(60\ min.\,s^{-1})}$$

$$= 8.0693 W$$

$$\eta = \frac{P_{ab}}{P_{hyd}}$$

$$= \frac{5.6542 W}{8.0693 W}$$

$$= 0.7007$$

For 1000 rpm

$$P_{ab} = \frac{n.M.2\pi}{60}$$

$$= \frac{(1000rpm)(0.054747Nm)(2\pi)}{60min.sec^{-1}}$$
$$= 5.7330W$$

$$P_{hyd} = \frac{Q.H}{1000.60}$$

$$= \frac{(35.0530l.min^{-1})(13826.01Pa)}{(1000min.m^{-3}).(60\ min.s^{-1})}$$
$$= 8.0773W$$

$$\eta = \frac{P_{ab}}{P_{hyd}}$$

$$= \frac{5.7330W}{8.0773W}$$
$$= 0.7097$$

For 1100 rpm

$$P_{ab} = \frac{n.M.2\pi}{60}$$

$$= \frac{(1100rpm)(0.049376Nm)(2\pi)}{60min.sec^{-1}}$$
$$= 5.6877W$$

$$P_{hyd} = \frac{Q.H}{1000.60}$$

$$= \frac{(35.0530 l. \, min^{-1})(13834.74 Pa)}{(1000 min. \, m^{-3}). \, (60 \, min. \, s^{-1})}$$

$$= 8.0824 W$$

$$\eta = \frac{P_{ab}}{P_{hyd}}$$

$$= \frac{5.6877 W}{8.0824 W}$$

$$= 0.7037$$

For 1200 rpm

$$P_{ab} = \frac{n. \, M. \, 2\pi}{60}$$

$$= \frac{(1200 rpm)(0.043678 Nm)(2\pi)}{60 min. \, sec^{-1}}$$

$$= 5.4875 W$$

$$P_{hyd} = \frac{Q. \, H}{1000.60}$$

$$= \frac{(35.0530 l. \, min^{-1})(13846.02 Pa)}{(1000 min. \, m^{-3}). \, (60 \, min. \, s^{-1})}$$

$$= 8.0890 W$$

$$\eta = \frac{P_{ab}}{P_{hyd}}$$

$$= \frac{5.4875 W}{8.0890 W}$$

$$= 0.6783$$

For 1300 rpm

$$P_{ab} = \frac{n.M.2\pi}{60}$$

$$= \frac{(1300rpm)(0.035679Nm)(2\pi)}{60min.sec^{-1}}$$

$$= 4.8571W$$

$$P_{hyd} = \frac{Q.H}{1000.60}$$

$$= \frac{(35.0530l.min^{-1})(13853.94Pa)}{(1000min.m^{-3}).(60\ min.s^{-1})}$$

$$= 8.0937W$$

$$\eta = \frac{P_{ab}}{P_{hyd}}$$

$$= \frac{4.8571W}{8.0937W}$$

$$= 0.6001$$

For 1400 rpm

$$P_{ab} = \frac{n.M.2\pi}{60}$$

$$= \frac{(1400rpm)(0.029539Nm)(2\pi)}{60min.sec^{-1}}$$

$$= 4.3306W$$

A deviation from formula (4.3) by considering pressure in Pa

$$P_{hyd} = \frac{Q.H}{1000.60}$$

$$= \frac{(35.0530 l.min^{-1})(13861.59 Pa)}{(1000 min.m^{-3}).(60\ min.s^{-1})}$$

$$= 8.0981 W$$

$$\eta = \frac{P_{ab}}{P_{hyd}}$$

$$= \frac{4.3306 W}{8.0981 W}$$

$$= 0.5347$$

For 1500 rpm

$$P_{ab} = \frac{n.M.2\pi}{60}$$

$$= \frac{(1500 rpm)(0.021832 Nm)(2\pi)}{60 min.sec^{-1}}$$

$$= 3.4293 W$$

$$P_{hyd} = \frac{Q.H}{1000.60}$$

$$= \frac{(35.0530 l.min^{-1})(13877.19 Pa)}{(1000 min.m^{-3}).(60\ min.s^{-1})}$$

$$= 8.1072 W$$

$$\eta = \frac{P_{ab}}{P_{hyd}}$$

$$= \frac{3.4293 W}{8.1072 W}$$

$$= 0.4229$$

For 1600 rpm

$$P_{ab} = \frac{n.M.2\pi}{60}$$

$$= \frac{(1600rpm)(0.010564m)(2\pi)}{60min.sec^{-1}}$$

$$= 1.7700W$$

$$P_{hyd} = \frac{Q.H}{1000.60}$$

$$= \frac{(35.0530l.min^{-1})(13883.23Pa)}{(1000min.m^{-3}).(60\ min.s^{-1})}$$

$$= 8.1108W$$

$$\eta = \frac{P_{ab}}{P_{hyd}}$$

$$= \frac{1.7700W}{8.1108W}$$

$$= 0.2182$$

For 1700 rpm

$$P_{ab} = \frac{n.M.2\pi}{60}$$

$$= \frac{(1700rpm)(0Nm)(2\pi)}{60min.sec^{-1}}$$

$$= 0W$$

$$P_{hyd} = \frac{Q.H}{1000.60}$$

$$= \frac{(35.0530 l.min^{-1})(13896.22 Pa)}{(1000 min.m^{-3}).(60\ min.s^{-1})}$$

$$= 8.1184W$$

$$\eta = \frac{P_{ab}}{P_{hyd}}$$

$$= \frac{0W}{8.1184W}$$

$$= 0$$

APPENDIX B

GANTT CHART

Gantt chart for PSM 1

Task \ Week	1	2	3	4	5	6	7	8	9	10	11	12	13	14	15	16
Project briefing by supervisor	■															
Making Introduction for the project		■	■													
Literature review study			■	■	■	■	■	■	■							
Methodology						■	■	■								
Manual experimentation								■	■	■	■					
CAD modeling									■	■	■	■				
Preparing for the proposal and Presentation slide											■	■	■			
Presentation for PSM														■		
Submit proposal															■	

Gantt chart for PSM 2

Task \ Week	1	2	3	4	5	6	7	8	9	10	11	12	13	14	15	16
CFD Simulation	■	■	■													
Literature review study		■	■	■	■	■	■									
CFD Simulation result validation					■	■	■	■	■							
Study on flow characteristic						■	■	■	■	■						
Analysis of turbine parameter based on result								■	■	■	■	■				
PSM 2 full report and presentation preparation											■	■	■			
Presentation for PSM 2														■		
Submit full report															■	

APPENDIX C

SIMULATION OF FLUID FLOW INSIDE UMP'S FRANCIS TURBINE USING COMPUTATIONAL FLUID DYNAMICS (CFD)

Muhammad Nur Iznei Bin Hashim, Devarajan a/l Ramasamy

Faculty of Mechanical Engineering, Universiti Malaysia Pahang,

26300 UMP, Kuantan, Pahang, Malaysia, Phone: +609-5492223 Fax: +609-5492244.

E-mail: muhdnuriznei@gmail.com, deva@ump.edu.my

ABSTRACT

This paper describes the fluid flow characteristic within a Francis Turbine using Computational Fluid Dynamics (CFD) simulation. The process is divided into 3 main parts that are experimentation, Computer-Aided Design (CAD) modeling, and CFD simulation. The experimentation is to obtain real data and measurement that will be used to validate the simulation data and to obtain boundary, initial, and working conditions of the Francis Turbine. CAD modeling is where the Francis Turbine is modeled with respect to the working part and fluid flow region. The last part is CFD simulation where the fluid flow is simulated and fluid flow data and characteristic is obtained. This paper provides complete fluid flow characteristic within the entire fluid flow of a Francis Turbine where earlier studies only concentrate on certain part of the turbine. This study will enable the analysis of fluid movement and its effect on efficiency which can then be used to improve the efficiency of the Francis Turbine.

KEYWORDS

Modeling simulation, CFD, Francis Turbine

1. Introduction

Francis turbine is a type of hydropower reaction turbine that contains a runner that has water passages through it formed by curved vanes or blades. As the water passes through the runner and over the curved surfaces, it causes rotation of the runner. The rotational motion is transmitted by a shaft to a generator. It is an inward flow reaction turbine that combines radial and axial flow concepts where both concepts are flow are integrated into the turbine in order to make the water flow within the generator to be able to generate highly efficient rotation and energy transfer to the shaft and runners. The fluid flow conditions within the entire region of the Francis Turbine are not investigated in most analysis since the main focus is always on the guiding vanes and runner where the energy is transferred to the driving shaft at these critical regions thus the lack in fluid flow result in the entire turbine. The objective of this paper is to create a CAD solid modeling of the Francis Turbine, run the model through CFD to obtain simulation data which will then be validated by results from experiment and to analyze the fluid flow characteristic data obtained from simulation.

2. Body of Paper

Model

For modeling and experimental purposes, the GUNT HAMBURG HM 150.20 demonstration Francis Turbine was chosen as the test model since the brand is well known for accuracy and reliability.

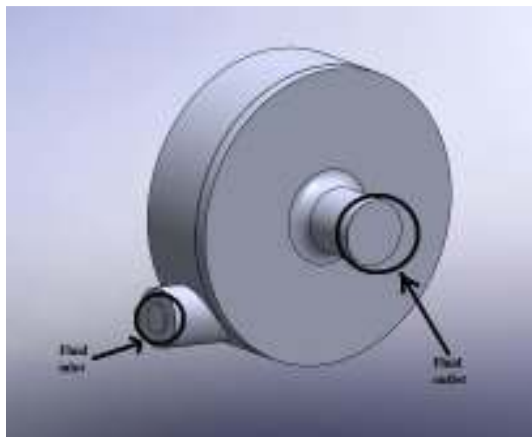**Figure 2.1:** Gunt Hamburg Demonstration Francis Turbine HM150.20

Figure 2.2: CAD model of the selected Francis Turbine with reference to working part
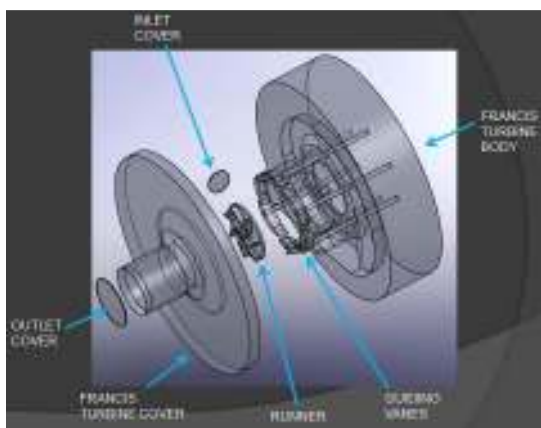

Figure 2.3 Exploded view of the CAD model with label by part

Experiment Procedure

1. Turbine characteristic curve

    vi. The guiding vanes were set up to maximum speed position to record turbine characteristic graph. The nominal angle of entrance was set to the usual 10-30°. However, the angle depends on the condition of the outlet flow, if cavities occur the angle needs to be adjusted so that the cavity will be eliminated.

    vii. The speed was measured with mounted tachometer which is mounted at the face of the pulley and reads the speed based on the metal object placed on the pulley and the lever was tightened to set the adjustment. The lever was tightened so that the guiding vanes will not move or sway at the power

of the flowing water running through the vanes.

    viii. Volumetric flow was set up to ~35 liter/min as described in the HM150 manual. The volume flow rate is measured to be ~35 liter/min, any adjustment need to be done before the experiment is done on the Francis Turbine. The entire series of measurements can be assumed volumetric flow rate as constant. Even though the value in actual does not flow at a constant rate due to the fluctuating pump, the value of the fluctuation is small and can be considered negligible since its effect on the reading is not significant and only occur a small time intervals.

    ix. The load at brake or the braking force is increased gradually to reduce the rpm to ~100rpm until the turbines speed declines and the runner finally stops. The braking force is adjusted by rotating the hand wheel on top of the braking unit. The braking force is then measured by calculating the difference between the reading of the right and left hand side force indicated.

    x. The reading of inlet pressure at each braking force increment is tabulated into a graph. After the braking force is applied and the pressure is stable, the reading of the pressure is taken. The reading was taken after the pressure is stable because the reading will be biased if taken immediately and to allow the system to properly adjust to the speed change.

2. Determination of flow rate,

    vii. The pump was turned on and the entire cycle of flowing water was left to flow for several moments. This is to allow the pump to build up its pressure and allow the water cycle to achieve stability before the reading can be taken.

    viii. Stop watch was set to zero. This is a pre-caution step to avoid error in reading due to human factors that is unable to response to the nature correctly.

    ix. The valve at bottom of volumetric tank is closed using a stopper. This

is to measure the volume flow rate of water running from the outlet of the Francis Turbine. This volume flow rate is to be considering constant the entire experiment process and constant in the inlet and outlet of the Francis Turbine.

x. Wait until the reading on the stop watch has reached 60 second or the water level at the volume indicator reaches 10L then start the stop watch reading. This is to allow the measure to be taken at a stable data and avoid zero error from the water scale.

xi. The time readings were taken after the water level has reached 20L and stop the stopwatch afterwards.

xii. 5 readings were taken and an average volume flow rate was calculated.

Computer-Aided Design (CAD) Modeling

1. Rough sketches were made using the dimensions taken to ensure that the model to be constructed in CAD is well visualize.
2. The Francis Turbine was constructed by parts according to their difficulty and the function of the parts and in the order of modeling is the turbine body, runner and the cover of the turbine.
3. The construction is done by with the dimension provided by the turbine manufacturer and cross-referencing it with the additional dimension obtained by mean of manual measurement on the turbine before experiment process.
4. After each part was constructed, the model is assembled into a complete Francis Turbine and the connection joint condition is checked to assure that it follows the actual working condition of a Francis Turbine.

Computational Fluid Dynamics (CFD) Simulation

1. The assembled Francis Turbine model will be opened in CFD and the simulation project for the simulation will be specified based on criteria identified important in the simulation such as surface roughness, units, fluid, physical feature etc.
2. The connection of the assembly was checked for interference and error to

avoid the simulation result from being biased.

3. In order to start the simulation, a new project is specified where the parameters are set.

Table 2.1 Project definition for the simulation

Project name	NEW: Francis Turbine
Unit system	SI
Analysis type	Internal; Exclude cavities without flow conditions
Physical features	Rotation: Type - Global rotating, Rotation axis - Z axis of Global Coordinate system, Angular velocity=0 RPM
Default fluid	Water
Wall Conditions	Adiabatic wall, default smooth walls
Initial Conditions	Default conditions
Result and Geometry Resolution	Set the Result resolution level to 4; Minimum gap size = 0.01 m, minimum wall thickness = 0.01, other options are default

Source: COSMOS Flow simulation

4. Then the boundary condition at the inlet and outlet will be subjected to the model in term of volume or mass flow rate and pressure. These values are obtained from the experimentation. The average value of the volume flow rate was measured during to be 35.0530 l/min and the flow is assumed to have uniform velocity profile with absolute value. The outlet is set to environmental pressure since in actual turbine water from the outlet will flow into open tank. Then is to set the rotating speed of the runner starting from 0 rpm to 1000 rpm with 100 rpm increment as obtained from experiment. The surfaces are selected and the boundary option is selected in order to specify each condition inside the turbine's fluid flow region.
5. Next is the identification of the turbine's body where a part of the turbine remains stationary such as the guiding vanes and internal wall is identified. The entire fluid contact surface of the turbine is set as stationary except for the runner. To specify the part as fixed, the surfaces are identified as real wall and stator.

6. After that is to specify the project goals and parameter at surfaces and parameters relevant to the study plus the equations for the goals specified. The goals set are at the inlet where the average pressure is measured, at the runner where the torque goal is specified a global goal for density

7. After the entire step has been completed, the simulation is started and the results will be obtained in a few hours after the COSMOS solver is finished calculating the flow conditions based on our earlier definitions, parameters, and data inputted into the simulation.

Result and discussion

1. Experiment result

Table 2.2: Flow data obtained from experiment

Speed, n (rpm)	Braking force, F (N)	Pressure Head, H (bar)	Torque at shaft, M (Nm)	Power at shaft, P_{ab} (W)	Hyd. Power, P_{hyd} (W)	Efficiency, η
1000	0.0	0.23	0.0000	0.0000	13.4390	0.0000
900	0.3	0.21	0.0075	0.0707	12.2685	0.0576
800	0.5	0.19	0.0125	1.0472	11.1001	0.0943
700	0.8	0.18	0.0200	1.4661	10.5159	0.1394
600	1.1	0.17	0.0275	1.7279	9.9317	0.1740
500	1.3	0.17	0.0325	1.7017	9.9317	0.1713
400	1.5	0.18	0.0375	1.5708	10.5159	0.1494
300	1.7	0.19	0.0425	1.3352	11.1001	0.1203
200	1.9	0.20	0.0475	0.9948	11.6483	0.0851
100	2.2	0.21	0.0550	0.5796	12.2685	0.0472
0	2.5	0.22	0.0625	0.0000	12.8528	0.0000

Source: Experimentation on Francis Turbine

Sample efficiency calculation for 0 rpm

$$M = \frac{F.D}{2}$$

$$= \frac{(2.5N).(0.05m)}{2}$$

$$= 0.0625 Nm$$

$$P_{ab} = \frac{n.M.2\pi}{60}$$

$$= \frac{(0rpm)(0.0625Nm)(2\pi)}{60}$$
$$= 0W$$

$$P_{hyd} = \frac{Q.H.10^5}{1000.60}$$

$$= \frac{(35.0530 l.min^{-1})(0.22bar)(10^5 Pa.bar^{-1})}{(1000 min.m^{-3}).(60\ min.s^{-1})}$$
$$= 12.8528 W$$

$$\eta = \frac{P_{ab}}{P_{hyd}}$$

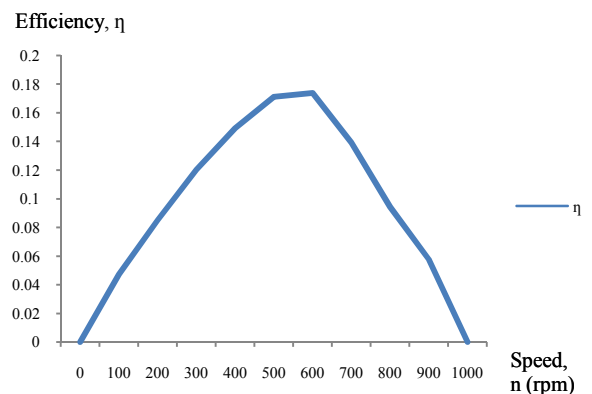$$= \frac{0W}{12.8528W}$$
$$= 0$$

Figure 2.4: Efficiency versus speed graph for experiment data

2. Simulation Result

Numerical Results

Table 2.3: Flow data obtained from COSMOS simulation for speed range 0- 1000rpm

Speed, n (rpm)	Inlet pressure, H (Pa)	Torque at shaft, M (Nm)	Power at shaft, P_{ab} (W)	Hyd. Power, P_{hyd} (W)	Efficiency, η
1000	13826.01	0.054747	5.7330	8.0773	0.7097
900	13812.23	0.059993	5.6542	8.0693	0.7007
800	13808.21	0.065789	5.5115	8.0669	0.6832
700	13819.18	0.072793	5.3360	8.0733	0.6609
600	13826.64	0.077814	4.8891	8.0777	0.6052

Speed (rpm)					
500	13831.06	0.079612	4.1684	8.0803	0.5158
400	13846.41	0.079618	3.3350	8.0893	0.4122
300	13853.95	0.083317	2.6174	8.0937	0.3233
200	13863.09	0.088432	1.8521	8.0990	0.2286
100	13871.45	0.091039	0.9533	8.1039	0.1176
0	13895.13	0.090652	0	8.1177	0

Source: COSMOS simulation

Sample efficiency calculation for 0 rpm

$$P_{ab} = \frac{n.M.2\pi}{60}$$

$$= \frac{(0rpm)(0.090652Nm)(2\pi)}{60}$$
$$= 0W$$

$$P_{hyd} = \frac{Q.H}{1000.60}$$

$$= \frac{(35.0530l.min^{-1})(13895.12Pa)}{(1000min.m^{-3}).(60\,min.s^{-1})}$$
$$= 8.1177W$$

$$\eta = \frac{P_{ab}}{P_{hyd}}$$

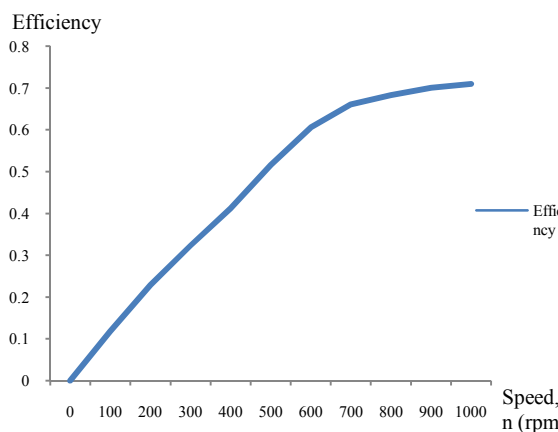$$= \frac{0W}{8.1177W}$$
$$= 0$$

Figure 2.5: Efficiency versus speed graph for simulation data for 0-1000rpm range

Considering the simulation curve only follows the experiment curve up to a certain

part, the simulation is continued by increasing the speed operating range.

Table 2.4: Flow data obtained from COSMOS simulation for speed range 0 - 1700rpm

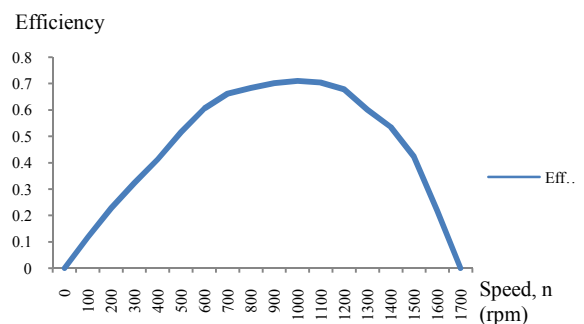| Speed, n (rpm)	Inlet pressure, H (Pa)	Torque at shaft, M (Nm)	Power at shaft, P_{ab} (W)	Hyd. Power, P_{hyd} (W)	Efficiency, η
1700	13896.22	0	0	8.1184	0
1600	13883.23	0.01056	1.7704	8.1108	0.2182
1500	13877.19	0.02183	3.4293	8.1072	0.4229
1400	13861.59	0.02953	4.3306	8.0981	0.5347
1300	13853.94	0.035679	4.8571	8.0937	0.6001
1200	13846.02	0.043678	5.4875	8.0890	0.6783
1100	13834.74	0.049376	5.6877	8.0824	0.7037
1000	13826.01	0.054747	5.7330	8.0773	0.7097
900	13812.23	0.059993	5.6542	8.0693	0.7007
800	13808.21	0.065789	5.5115	8.0669	0.6832
700	13819.18	0.072793	5.3360	8.0733	0.6609
600	13826.64	0.077814	4.8891	8.0777	0.6052
500	13831.06	0.079612	4.1684	8.0803	0.5158
400	13846.41	0.079618	3.3350	8.0893	0.4122
300	13853.95	0.083317	2.6174	8.0937	0.3233
200	13863.09	0.088432	1.8521	8.0990	0.2286
100	13871.45	0.091039	0.9533	8.1039	0.1176
0	13895.13	0.090652	0	8.1177	0

Source: COSMOS Flow simulation

Figure 2.6: Efficiency versus speed graph for simulation data for 0-1700rpm range

Graphical Results

Pressure

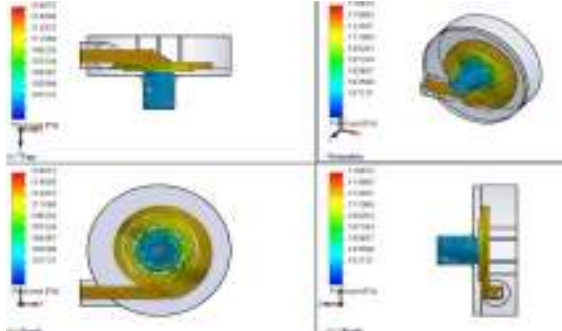**Pressure Flow Trajectories inside Fluid**

Figure 2.7: Pressure flow inside the fluid in Francis Turbine

As shown in Figure 2.7, the pressure of the fluid (water) inside the turbine is relatively constant with the fluid maintaining a steady pressure up to the fluids entrance through the guiding vanes to the runner. The reason for these is that the high pressure fluid transfers its kinetic energy to the runner as it passes through the runner and losses the energy which reduces the pressure of the fluid after the energy is transferred.

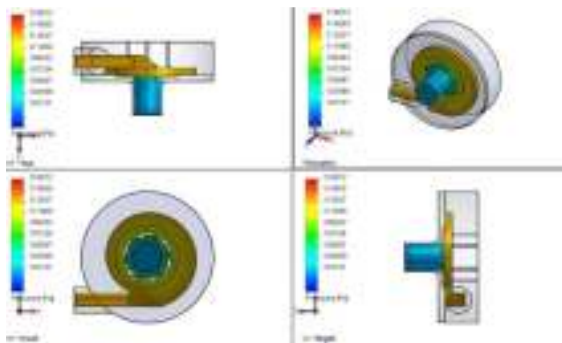**Pressure Contour on the Internal Surfaces of the Francis Turbine**

Figure 2.8: Pressure contour on the internal surfaces of the Francis Turbine

In Figure 2.8, it offers us with the pressure reading taken at all internal surfaces in contact with the fluid during simulation and gives us with the reading at all surfaces. With reference to these reading, we are able to make assumptions on how the fluid moves and whether there is part of the turbine which is subjected to extreme pressure and if there is any pressure build-up on the turbine's internal surfaces. If any pressure build-up I spotted, it

can be assumed as the turbine's weakest point and the first point which the turbine will fail first. However, as the simulation result shows, the pressure is evenly distributed and the turbine will less likely to fail at any specific location. By analyzing the pressure distribution on the internal surfaces, it is safe to assume that the fluid flow inside the turbine at the ambient and experiment condition to be turbulent.

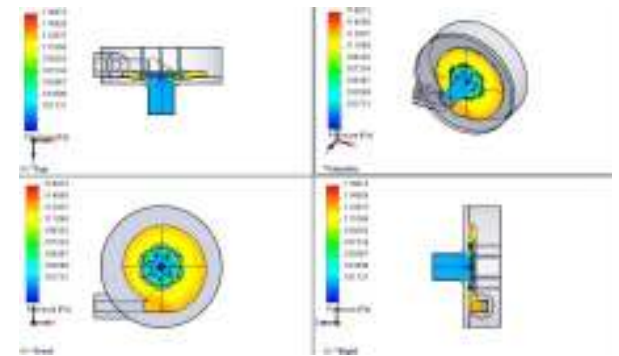**Pressure Contour Cut Plot inside Fluid Flow Region**

Figure 2.9: Pressure contour cut plot in the fluid flow region

In Figure 2.9, a pressure cut plot of the result is presented where the several cut shown is made parallel to each axis of the model that are the x, y, and z axis. By doing this we will be able to get a more detail view of the pressure distribution inside the turbine. As shown on the front view, our statement on the pressure loss as the energy was transferred to runner is clearly shown by the clear view of a large pressure drop on the turbines runner.

Velocity

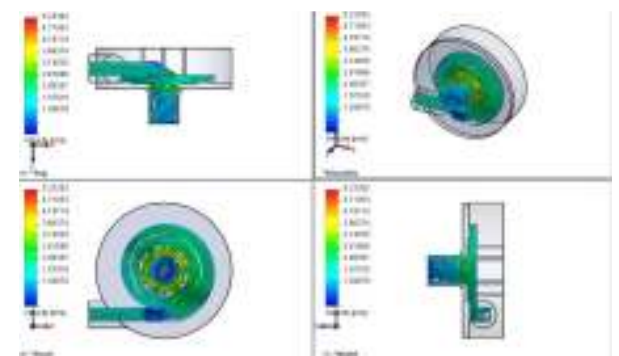**Velocity Flow Trajectories inside Fluid**

Figure 2.10: Pressure flow inside the fluid in Francis Turbine

In Figure 2.10 the velocity of the fluid flow inside the turbine is shown. It can be noted that velocity is relatively constant but there are several region where the velocity experience change whether increase or decrease. As shown in figure, the fluid velocity increases as the fluid passes through the guiding vanes and enters the runner. This can attributed to the movement of the runner as kinetic energy from the moving water is transferred to runner. The fluid speed then decreases as the fluid passes the runner and head through the outlet which due to the runner rotating as the effect of energy transferred to it and not the other way around. However, there is a peculiar pressure drop near the water entrance to the main part of the turbine which yields a warning in COSMOS Flow Simulation signaling that a water vortex has developed inside of the turbine.
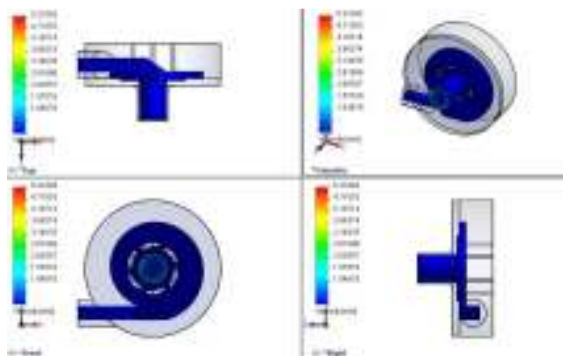
Velocity Contour on Turbine Internal Surfaces

Figure 2.11: Velocity contour on the internal surfaces of the Francis Turbine

In Figure 2.11, the fluid velocity on the turbine internal surfaces are shown to investigate the fluid characteristic around the internal surfaces of the turbine. In the figure, it is clearly shown that fluid flow on the internal surfaces of the turbine in constant with nearly no change what so ever in the velocity except for the slight increase at the outlet of the turbine. The vortex that exist earlier in the velocity fluid flow doesn't show any difference in the internal surface contour since the vortex that occurred has relatively the lowest velocity in the velocity fluid flow in figure 2.10. The constant velocity contour furthermore confirms the earlier statement of the fluid flow being turbulent throughout the entire turbine.

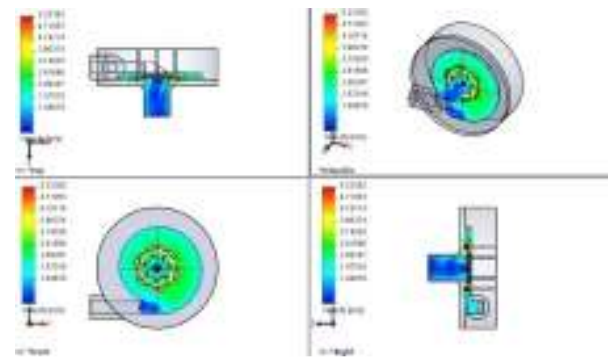**Velocity Contour Cut Plot inside Fluid Flow Region**

Figure 2.12: Velocity contour cut plot in the fluid flow region

The velocity contour cut plot inside fluid flow region shown in Figure 2.12 gives a clearer view of the fluid velocity in the fluid flow region of the turbine during operating condition. The figure shows that the velocity major increase is at the runner as shown in Figure 2.10 but there is also a slight increase as the fluid hits the wall of the turbine and moves to the runner of the turbine, the increase in fluid velocity is attributed to the molecular energy of water as the water particles collide with each other and the turbine wall.

This provides additional energy to the moving water in the sense of velocity increment. However due to the small energy gained as the result of these collisions, the increase in the fluid velocity is not really noticeable. In Figure 2.11, it is clearly shown that the vortex results in velocity drop in the main turbine compartment, however it is not known whether the presence of the vortex has any sort of huge effect on the fluid flow characteristic within the Francis Turbine.
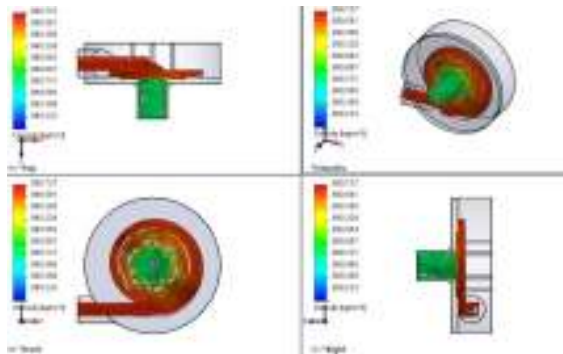
Density

Density flow Trajectories inside fluid

Figure 2.13: Density flow inside the fluid in Francis Turbine

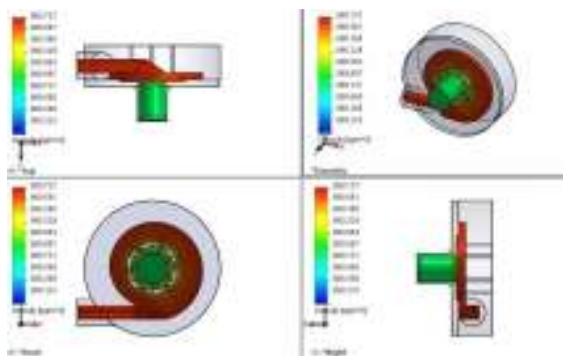**Density Contour on Turbine Internal Surfaces**

Figure 2.14: Density contour on the internal surfaces of the Francis Turbine

Both Figure 2.13 and 2.14 are used to evaluate whether cavitations occurs in the turbine. To identify if cavitations occurs, the result is analyzed to see whether there is any sudden density drop in the turbine. During cavitations occurrence, bubbles filled with air forms around the guiding vanes and runner which result in runner and guiding vanes cracking. By identifying if there is density drop up to the density of air cavitations can be identified. However based on both figure there is no density drop to air density level which makes it safe to assume that cavitations doesn't occur in the simulation.

VALIDATION

The validation study as mention earlier is done by mean of comparing efficiency curve pattern. As shown in Figure 2.15, both figure exhibits similar pattern but with different graph

curve. Since the pattern is similar, the results are considered validated and reason of the values differences will be discussed on next sub-chapter.
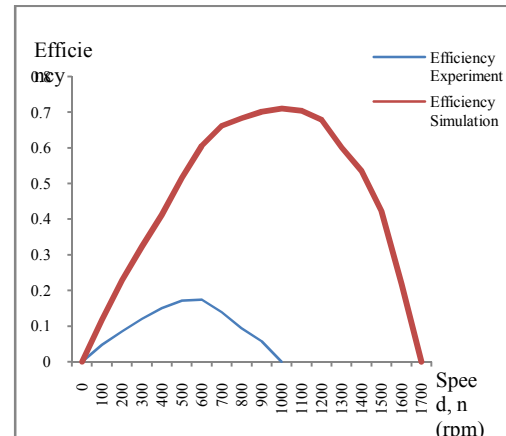

Figure 2.15: Efficiency versus speed graph for experiment and simulation data

$$\% = \frac{\eta \text{ simulation} - \eta \text{ experiment}}{\eta \text{ simulation}}$$

$$= \frac{0.7097 - 0.1740}{0.7097}$$
$$= 0.7548 @ 75.48\%$$

DISCUSSION

As observed from Table 2.2 and Figure 2.4, the efficiency value for the Gunt Hamburg Demonstration Francis Turbine obtained from experiment is rated at a mere 17 percent efficiency, a far cry from the theoretical value of 60–90 percent. The possible factors contributing these low efficiency values can be attributed to several factors. The main factor that was observed during experiment was the physical condition of the turbine itself.
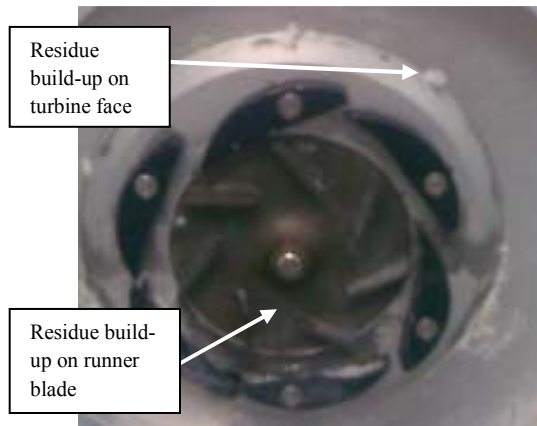
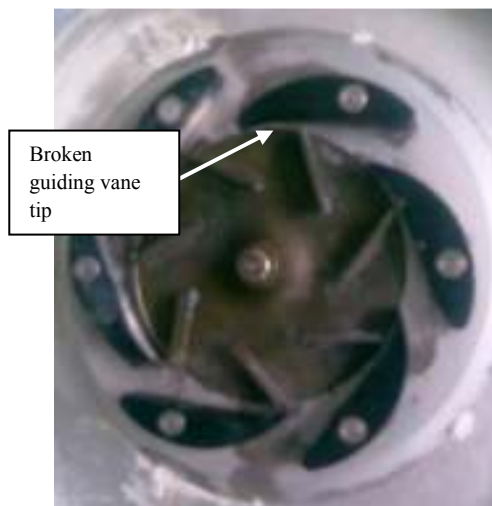**Figure 2.16:** Foreign build-up on turbine face

Figure 2.17: Guiding vanes disorientations

The Figure 2.16 and 2.17 shows the physical imperfection and damage to the physique of the turbine. The arrows in figure 2.16 points out to the foreign build-up of plaque caused from continuous usage of unclean water as the operating fluid. As pointed out by the arrows, the build-up center around the turbine's guiding vanes and runner which are the most critical part of the turbine. The formation of these build-up attribute to the loss of energy due to the friction between the flowing water with these build-up.

Next in Figure 2.17, the figure displays the disorientations of the guiding vanes with the vanes pointed by the arrow having the curvature tip broken. During pre-experimental process, we have tried to align the guiding vanes back to the original and correct vanes position but were failed by the aging components of the turbine which limits the amount of vanes correction done. To overcome this, the Turbine was left to

run and the vane angle was adjusted until the cavitations are decreased to the lowest possible. The angle is the taken as the average angle of all vane angles.

In the simulation, using the speed range obtained from the experiment we were not able to obtain the same efficiency curve as those obtained from experiment. This is attributed to the turbine age. The shaft which transfer torque from the runner to the flywheel has undergone numerous experimentation process which led to the wear and tear of the part. Furthermore, the continuous usage suggest that the increase in the surface roughness on the shaft and the contacting surface. Including these factors in the assumption, it can be estimated that the energy transferred to the flywheel is lost at the shaft resulting in the decrease in operating speed range since energy is lost from the runner during transfer process.

In the simulation, the maximum value of efficiency rated is around 70 percent where as the theoretical efficiency value is around 90 percent. The reason for this is that the theoretical is the estimated efficiency value for the normal conventional Francis Turbines used in dam where the energy obtained from the is obtained from both radial and axial flow where as the Francis Turbine of interest only gain energy from axial flow. This alone explains the reason why the efficiency of the simulation only reaches 70 percent.

Due to the geometric design of the Francis Turbine a water vortex gathers at the inlet of the main body of the Francis Turbine. The fluid at this region seems to have similar pressure to the surrounding fluid but sport and obvious drop in velocity. This phenomenon may at first seem to affect the reading of the turbine but upon closer inspection at Figure 2.12 it can noticed that the vortex region does not restrict flow as it only gather at the front part of the water entrance.

3. Conclusion

In conclusion the paper is was able to obtain graphical data on flow characteristic within the entire fluid flow region of the selected Francis Turbine model. All of the result incorporating fluid flow characteristic in term of the entire fluid flow region was displayed with reference to velocity and pressure flow trajectories, surface contour and surface contour cut-plot. The advantages of using flow simulation rather than obtaining it from

experimentation is that simulation consume less time is able to provide direct graphical result of the fluid flow where as experiment data need to be processed in order to obtain graphical result. However using simulation also have some limitation such in our case that the for the result concise, high mesh density needs to be selected and such settings will require higher time than experiment, next is that the simulation only varies certain parameters where there are more parameters to be considered in order for accurate result. The result in this paper can be continued in further research for efficiency improvement, design optimization and flow movement analysis.

References

[1] Qian Z. D., Yang J. D., Huai W. X. 2006. Numerical simulation and analysis of pressure pulsation in Francis Hydraulic Turbine with air admission.

[2] Xiao R., Wang Z. W., Luo Y. Y. 2008. Dynamic Stresses in a Francis Turbine Runner Based on Fluid-Structure Interaction Analysis.

[3] Ruixia Q. 2008. Flow Field Measurements in a distributor of a Francis Turbine.

[4] Zhang L. X., Wang W. Q . 2006. Intrinsic features of turbulent flow in strongly 3-D skew blade passage of a Francis Turbine.

[5] Marjavaara, B. D. 2004. CFD Driven Optimization of Hydraulic Turbine Draft Tubes using Surrogate Models.

[6] Eerle, P., Couston, M. and Sabourin, M. 2002. Refurbishment of low head Francis Turbines, Proceedings of the XXIst IAHR Symposium on Hydraulic Machinery and Systems (ed. F. Avellan, G. Ciocan and S. Kvicinsky) IAHR, Lausanne.

[7] Avellan, F. 2000 Flow Investigation in a Francis Draft Tube: the FLINDT Project, Proceedings of 20th IAHR Symposium on Hydraulic Machinery and System.

[8] Marjavaara, B. D. 2004. Parameterization and Flow Design Optimization of Hydraulic Turbine Draft Tubes, Licentiate Thesis, Luleå University of Technology.

[9] Guo P. C., Luo X. Q., Zheng X. B. et al. 2006. Numerical investigation of three-dimension turbulent flow fields in a Francis turbine.

[10] Shao Q., Liu S. H., Wu Y. L. et al. 2004. Three-dimensional simulation of unsteady flow in model Francis hydraulic turbine.

[11] Zhang K. W. et al. 2005. Study on PIV measurement of exit velocity distribution of Francis turbine runner.

[12] Mufeed O. 1999. A Summary of Environmentally Friendly Turbine Design Concept.